

**The Islamic University–Gaza**  
**Research and Postgraduate Affairs**  
**Faculty of Science**  
**Master of Physics**



الجامعة الإسلامية - غزة  
شئون البحث العلمي والدراسات العليا  
كلية العلوم  
ماجستير الفيزياء

## **Improvement of electric and magnetic properties for Li spinel ferrite by divalent Ni<sup>2+</sup> ions substitution**

تأثير أيونات النيكل الثنائية على الخواص الكهربائية والمغناطيسية  
لليثيوم اسبنل فيريت

**Elham Abed Alfattah Elhillo**

**Supervised by:**

**Dr. Hussain Dawoud**

**Associate Professor of Physics**

**A thesis submitted to the Faculty of Science as a partial fulfilment of the  
requirements for the degree of Master of Science in Physics**

**July/2017**

## إقرار

أنا الموقع أدناه مقدم الرسالة التي تحمل العنوان:

### **Improvement of electric and magnetic properties for Li spinel ferrite by divalent Ni<sup>2+</sup> ions substitution**

### **تأثير أيونات النيكل الثنائية على الخواص الكهربائية والمغناطيسية لليثيوم اسبنل فريت**

أقر بأن ما اشتملت عليه هذه الرسالة إنما هو نتاج جهدي الخاص، باستثناء ما تمت الإشارة إليه حيثما ورد، وأن هذه الرسالة ككل أو أي جزء منها لم يقدم من قبل الآخرين لنيل درجة أو لقب علمي أو بحثي لدى أي مؤسسة تعليمية أو بحثية أخرى.

### **Declaration**

I understand the nature of plagiarism, and I am aware of the University's policy on this.

The work provided in this thesis, unless otherwise referenced, is the researcher's own work, and has not been submitted by others elsewhere for any other degree or qualification.

Student's name:

الهام عبد الفتاح الحلو

اسم الطالب

Signature:

التوقيع:

Date:

التاريخ:



الرقم: ج س غ/35/ Ref:

التاريخ: 15/08/2017 Date:

## نتيجة الحكم على أطروحة ماجستير

بناءً على موافقة شئون البحث العلمي والدراسات العليا بالجامعة الإسلامية بغزة على تشكيل لجنة الحكم على أطروحة الباحثة/ الهام عبدالفتاح ابراهيم الحلو لنيل درجة الماجستير في كلية العلوم قسم الفيزياء وموضوعها:

### تأثير أيونات النيكل الثنائية على الخواص الكهربائية والمغناطيسية لليثيوم اسبنل فيريت Improvement of electric and magnetic properties for Li spinel ferrite by divalent Ni<sup>2+</sup> ions substitution

وبعد المناقشة العلنية التي تمت اليوم الثلاثاء 23 ذو القعدة 1438هـ، الموافق 2017/08/15م الساعة الحادية عشر صباحاً، اجتمعت لجنة الحكم على الأطروحة والمكونة من:

د. حسين عبد الكريم داود مشرفاً ورئيساً  
د. سفيان عبد الرحمن تايه مناقشاً داخلياً  
د. مجدي سالم حمادة مناقشاً خارجياً

وبعد المداولة أوصت اللجنة بمنح الباحثة درجة الماجستير في كلية العلوم/ قسم الفيزياء. واللجنة إذ تمنحها هذه الدرجة فإنها توصيها بتقوى الله ولزوم طاعته وأن تسخر علمها في خدمة دينها ووطنها.

والله ولي التوفيق،،،

نائب الرئيس لشئون البحث العلمي والدراسات العليا

أ.د. عبدالرؤوف علي المناعمة



## Abstract

In the present work magnetic, electric and dielectric properties are investigated for mixed ferrite  $Li_{0.5(1-x)}Ni_xFe_{2.5-0.5x}O_4$  ( where  $x=0.0, 0.2, 0.4, 0.6, 0.8$  and  $1.0$ ) which are prepared from high purity oxides using standard ceramic technique. The net magnetization ( $M$ ) was measured at room temperature in the range of the applied field [200-2650 (A/m)]. The results indicated that the  $M$  decreased with increasing of the  $Ni^{2+}$  ions. The highest value of  $M$  was registered for the sample of  $x=0.0$ , where the lowest value was registered for the samples of  $x=1.0$ . The inductance was measured as a function of temperature to determine the Curie temperature  $T_C$  (It is the temperature which the material transform from ferrimagnetic to paramagnetic . It was found that, the Curie temperature  $T_C$  decreased with increasing of the  $Ni^{2+}$  ions. Complex dielectric constant ( $\epsilon^*$ ), dielectric loss tangent ( $\tan\delta$ ) and AC conductivity ( $\sigma_{AC}$ ) were investigated in the frequency range of  $(10^4 - 10^6)Hz$  at room temperature. It was found that, the  $\epsilon^*$  and  $\tan\delta$  were decreased continuously, while  $\sigma_{AC}$  was increased with increasing of the applied frequency.

## المخلص

في هذا البحث تم دراسة الخواص المغناطيسية والكهربائية بالإضافة الى خواص العزل الكهربائي والموصلية في حالة التيار المتردد لمركب ليثيوم -نكل فريت حسب الصيغة  $(Li_{0.5(1-x)}Ni_xFe_{2.5-0.5x}O_4)$  الذي تم تحضيره من أكاسيد عالية النقاء باستخدام الطريقة السيراميكية القياسية، حيث  $(x= 0.0, 0.2, 0.4, 0.6, 0.8 \& 1)$ .  
تم قياس المغنطة ( $M$ ) عند درجة حرارة الغرفة في مجال مغناطيسي متغير  $(200 \text{ to } 2650) A.m^{-1}$  ووضحت النتائج ان المغنطة تقل بزيادة تركيز أيونات النيكل في العينات. حيث انه عندما تكون تركيز ايونات النيكل  $x=0.0$  تكون أعلى قيمة للمغنطة ، وعندما تكون تركيز ايونات النيكل يساوي 1.0 تكون أقل قيمة للمغنطة .  
لقياس درجة كوري (درجة الحرارة التي عندها تتحول المادة من فري الى بارا ) تم قياس محاثة الملف كدالة في درجة الحرارة وقد وجد انها تقل بزيادة تركيز أيونات النيكل .  
تم حساب ثابت العزل ( $\epsilon$ ) وثابت الفقد ( $\tan \delta$ ) والموصلية في حالة التيار المتردد ( $\sigma_{AC}$ ) في ترددات ضمن مدى  $(10^4 - 10^6) Hz$  في درجة حرارة الغرفة ، وقد وجد ان قيمة  $\epsilon$  , ( $\tan \delta$ ) تقل بزيادة التردد ، بينما تزداد قيمة  $\sigma_{AC}$  بزيادة التردد .

## **Dedication**

*This thesis work is, specially, dedicated*

*To*

*The continuous source of support, may Allah , my lovely mother*

*To*

*My lovely father,*

*To*

*My husband and my baby*

*To*

*My brothers and sisters*

*And*

*To all whom have always loved me unconditionally and taught me how to  
work hard for things that I aspire to achieve.*

## **Acknowledgment**

*This thesis becomes a reality with the kind support and help of many individuals. I would like to extend my sincere thanks to all of them.*

*Foremost, I want to offer this success to our GOD Almighty for the wisdom he bestowed upon me, the strength, peace of my mind and good health in order to finish this thesis.*

*I would like to express my special gratitude and thanks to my adviser **Dr. Hussain Dawoud**. May Allah bless him, for imparting his knowledge and experiences in this study, which would not have been completed without him.*

*I am highly indebted to Physics Department-Faculty of Science in Islamic University of Gaza for their guidance and constant supervision as well as for their support in my study years.*

*My thanks and appreciation also go to my lovely family, my teachers and friends in all sides of my life for giving me their love, kind wishes, advices and beautifies my life.*

## Table of Contents

<b>Declaration .....</b>	<b>I</b>
<b>Abstract.....</b>	<b>II</b>
<b>Dedication.....</b>	<b>IV</b>
<b>Acknowledgment.....</b>	<b>V</b>
<b>Table of Contents.....</b>	<b>VI</b>
<b>List of Tables .....</b>	<b>VIII</b>
<b>List of Figures.....</b>	<b>IX</b>
<b>Introduction.....</b>	<b>1</b>
<b>CHAPTER 1 : Theoretical Background.....</b>	<b>8</b>
1.1 Structure of Spinel Ferrite Materials .....	9
1.1.1 Spinel Lattice Structure .....	9
1.1.2 Types of Spinel Lattice Structure .....	11
1.1.3 The Factors that effect on the structure.....	12
1.2 Magnetic Properties of the Ferrimagnetic Materials .....	13
1.2.1 Magnetization Process of the Ferrimagnetic Materials .....	14
1.2.2 Ferrimagnetic Domains.....	15
1.2.3 Molecular Field Theory of the Ferrimagnetic Materials .....	16
1.3 Electric Properties of the Ferrimagnetic Materials .....	20
1.3.1 Conductivity of the Ferrimagnetic Materials.....	20
1.3.2 Conduction Mechanism in the Ferrimagnetic Materials.....	21
1.4 Dielectric Properties of the Ferrimagnetic Materials.....	22
<b>CHAPTER 2 : Literature Survey.....</b>	<b>24</b>
2.1 Magnetic Properties .....	25
2.2 Electric Properties.....	26
2.3 Dielectric Properties .....	26
<b>CHAPTER 3 : Experimental Techniques.....</b>	<b>28</b>
3.1 Preparation of Samples .....	29
3.2 Characterization of the Magnetic Properties.....	30
3.3 Determination of Curie Point Temperature .....	32



3.4 Characterization of the AC Conductivity and Dielectric Properties.....	33
<b>CHAPTER 4 : Results and Discussion.....</b>	<b>35</b>
4.1 Magnetic Properties .....	36
4.1.1 Magnetic Moment.....	36
4.1.2 Ionic radii for Tetrahedral and Octahedral Sites.....	37
4.1.3 Magnetization Study .....	38
4.1.4 Relative Permeability.....	40
4.2 Electric Properties.....	41
4.3 Dielectric Properties .....	44
4.4 AC Conductivity .....	47
<b>Conclusion .....</b>	<b>49</b>
<b>References.....</b>	<b>51</b>

## List of Tables

<b>Table (1.1):</b> Various possibilities of the ionic charge distribution of the cations of the spinel lattice structure.....	11
<b>Table (3.1):</b> Weight of each oxide used to prepare the various samples for the mixed <i>Li-Ni</i> spinel ferrite.....	29

## List of Figures

<b>Figure (1.1):</b> Classification of the magnetic materials.....	3
<b>Figure (1.2):</b> Two octants of the unit cell of the spinel lattice structure $A$ ions are at $T_d$ sites and $B$ ions are at $O_h$ sites of the $Z^{2-}$ anions packing.....	10
<b>Figure (1.3):</b> An anion $Z^{2-}$ in the spinel lattice structure with its nearest cations neighbors.....	10
<b>Figure (1.4):</b> Spins distribution at $T_d$ and $O_h$ sites.....	13
<b>Figure (1.5):</b> Superexchange interactions between the anions, $O^{2-}$ ions, and the cations, the $T_d$ and the $O_h$ sites.....	14
<b>Figure (1.6):</b> Alignment of Weiss domains.....	16
<b>Figure (1.7):</b> Inverse magnetic susceptibility of the ferrimagnetic materials above the $T_C$ according to the molecular field theory.....	20
<b>Figure (3.1):</b> A toroidal sample shape.....	31
<b>Figure (3.2):</b> Circuit diagram for measuring the magnetization using the toroidal samples of the mixed $Li-Ni$ spinel ferrite.....	32
<b>Figure (3.3):</b> Circuit diagram for measuring the inductance of the toroidal samples of the mixed $Li-Ni$ spinel ferrite.....	33
<b>Figure (4.1):</b> Variation of $\mu_o$ , $\mu_T$ and $\mu_{net}$ with the $Ni^{2+}$ ratio.....	37
<b>Figure (4.2):</b> Variation of $R_T$ and $R_O$ with the $Ni^{2+}$ ratio.....	38
<b>Figure. (4.3):</b> Variation of $M$ with $H$ for the samples with $x = 0.0, 0.2, 0.4, 0.6, 0.8$ and $1.0$ .....	39
<b>Figure (4.4):</b> Variation of $\mu_r$ with $H$ for the samples with $x = 0.0, 0.2, 0.4, 0.6, 0.8$ and $1.0$ .....	40
<b>Figure (4.5a):</b> Variation of induction $L$ with temperature for samples of $x = 0.0, 0.2$ and $0.4$ .....	43

<b>Figure (4.5b):</b> Variation of induction L with temperature for samples of x = 0.6, 0.8 and 1 .....	43
<b>Figure (4.6):</b> Variation of $T_c$ with $Ni^{2+}$ ratio.....	44
<b>Figure (4.7):</b> Variation of absolute value of $\varepsilon^*$ against the applied frequency for the samples with x = 0.0, 0.2, 0.4, 0.6, 0.8 and 1.0 at room temperature.....	46
<b>Figure (4.8):</b> Variation of $\tan \delta$ against the applied frequency for the samples with x = 0.0, 0.2, 0.4, 0.6, 0.8 and 1.0 at room temperature.....	46
<b>Figure (4.9):</b> Variation of $\sigma_{AC}$ against the applied frequency for the samples with x = 0.0, 0.2, 0.4, 0.6, 0.8 and 1.0 at room temperature.....	48

# **Introduction**

## Introduction

Materials are called magnetic materials when they are magnetized by a magnetic field. The intensity of the intrinsic magnetization of the magnetic substance  $M$  is defined as the magnetic moment  $\mu_{net}$  per unit volume of the magnetic substance (Rudden and Wilson, 1984). Materials can be classified in terms of their magnetic behaviour, depending on their magnetic susceptibility  $\chi_m$  values, which change with the applied magnetic field intensity as well as temperature, into one of five groups diamagnetic, paramagnetic, ferromagnetic, antiferromagnetic and ferrimagnetic (Chikazumi, 1964). These groups are illustrated in figure (1.1).

### i. Diamagnetism

Diamagnetism is described for the materials that have a very weak magnetism that results from changes induced in the orbits of electrons in the atoms of a substance by an external magnetic field. They are composed of the atoms which have no net magnetic moment. However, when they expose to an external field, their  $M$  acts in the opposite direction of the applied magnetic field  $H$  then a negative magnetization is produced and thus; the magnetic susceptibility is negative ( $\chi_m < 0$ ).

### ii. Paramagnetism

In paramagnetism, some of the atoms or ions of the substance have a net orbital or spin magnetic moments due to unpaired electrons in partially filled orbitals. In the presence of an external magnetic field, there is a partial alignment of the magnetic moments in the direction of the field resulting in a net small, positive susceptibility ( $\chi_m > 0$ ), when the field is removed the magnetization is zero .

### iii. Ferromagnetism

Ferromagnetic materials have some unpaired electrons so their atoms have  $\mu_{net}$ . Ferromagnetism is described for the materials which their spins are aligned parallel to each other when applied an external magnetic field such that alignment is almost complete over small regions with a particular overall spin orientation are termed domains. This strong spin alignment leads ferromagnetic materials to have a large,

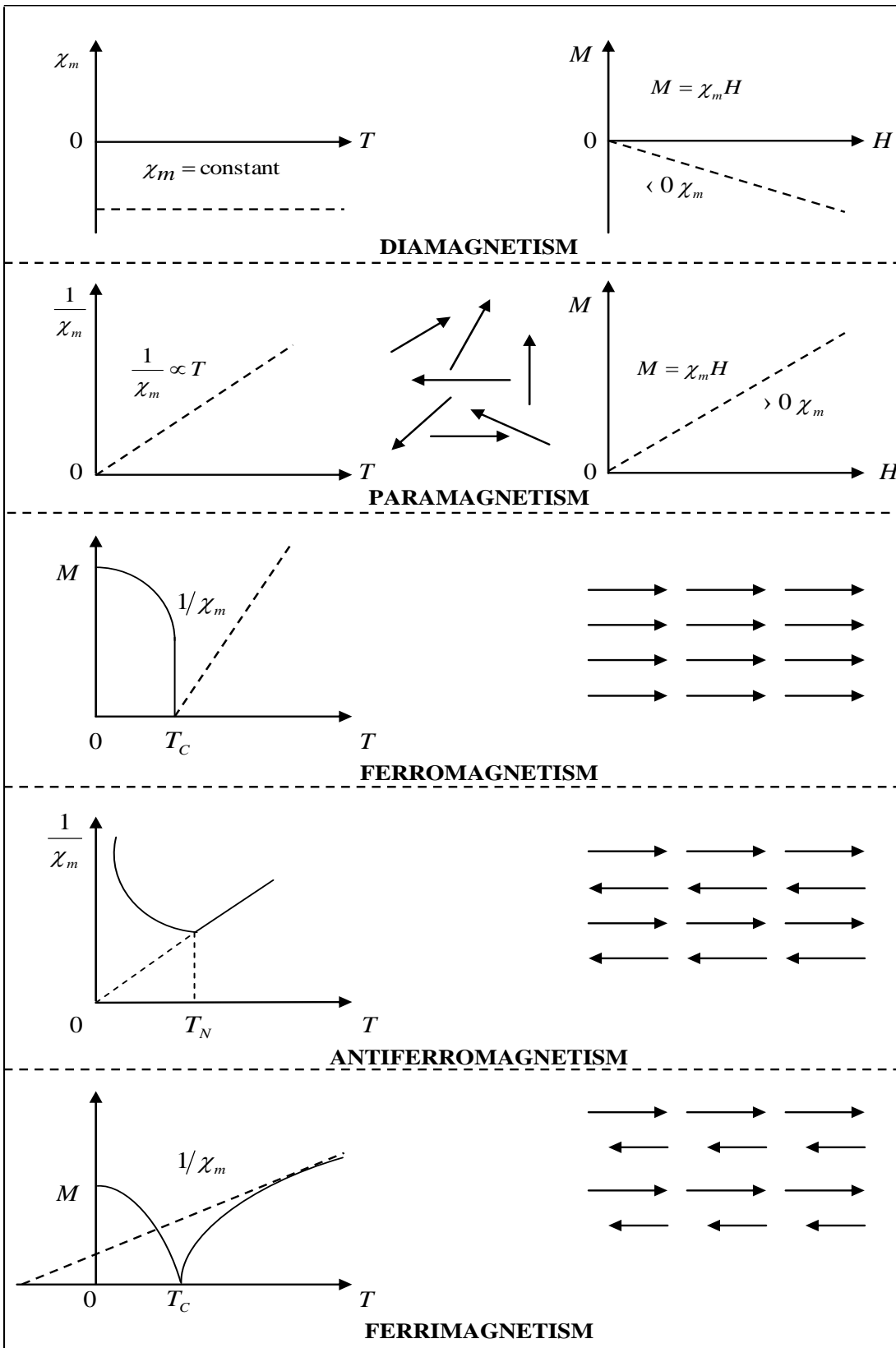


Fig. (1-1): Classification of the magnetic materials.

positive susceptibility. They exhibit a strong attraction to magnetic fields and are able to retain their magnetic properties after the external field has been removed. Above a critical temperature, called Curie temperature point  $T_C$ , the thermal motion is sufficient to offset the aligning force and the material becomes paramagnetic.

#### **iv. Antiferromagnetism**

Antiferromagnetism is described for the materials which have a weak magnetism. It is exhibiting a small, positive magnetic susceptibility. The simplest model structure of these materials consists of two magnetic sublattices with the same magnetic moments, thus; their net magnet moment is zero. The individual magnetic moments on each sublattice are aligned ferromagnetically with antiparallel coupling between the two magnetic sublattices. Above a critical temperature, called Neel's temperature point  $T_N$ , thermal energy is sufficient to disorder the individual magnetic moments in antiferromagnetic materials which become paramagnetic.

#### **v. Ferrimagnetism**

The structure of the ferrimagnetic materials is composed of more than two magnetic sublattices which are separated by oxygen ions. Therefore, the exchange interactions are mediated by the anions (oxygen,  $O^{2-}$  ions). When this happens, the interactions are called indirect or superexchange interactions.

The strongest interactions tend to an antiparallel alignment of the spins between the two sublattices. In these materials, the magnetic moments for the two sublattices are not the same, so the net magnetization of these materials is not zero. Their magnetic moments disappear above Curie temperature point  $T_C$  at which the thermal energy randomizes the individual magnetic moments and then these materials become paramagnetic. The colour of this material varies from silver grey to black.

#### **Classification of Ferrimagnetic Materials**

Ferrites are dark brown or grey in appearance and very hard and brittle in physical character. They are prepared by heat-treating the various transition metal oxides or alkaline earth oxides with the ferric oxides (Snoek, 1947). There are many compounds



of these materials, which classified in term of either their crystal structure or their applications.

### **1. According to the crystal structure**

There are many compounds of these materials which classified by a term descriptive of their crystal structure. These types are (Morrish, 1965)

- i. Ferrimagnetic spinel materials in the form  $MeFe_2O_4$  , where  $Me$  is a divalent metal atom of the same type, which may be either magnetic or non-magnetic, such as  $Ni$ ,  $Zn$ ,  $Cu$ ,  $Fe$ ,  $Co$ ,  $Mn$ ,  $Mg$  or  $Cd$  , e.g. nickel ferrite  $NiFe_2O_4$  and zinc ferrite  $ZnFe_2O_4$  also, their combination, e.g. the mixed  $Ni$ -  $Zn$  spinel ferrite.
- ii. Hexagonal oxides in the form  $MeFe_{12}O_{19}$ , where  $Me$  such as  $Ba$ ,  $Sr$ ,  $Pb$  and their combination, e.g. barium ferrite  $BaFe_{12}O_{19}$ .
- iii. Ferrimagnetic garnet materials in the form  $U_3Fe_5O_{12}$ , where  $U$  is replaced by the trivalent rare earth ions, such as  $Y$ ,  $Pm$ ,  $Sm$ ,  $Eu$ ,  $Gd$ ,  $Tb$ ,  $Dy$ ,  $Ho$ ,  $Er$ ,  $Tm$ ,  $Yb$  or  $Lu$ . The rare earth garnets are commonly called RIG's. The commonly example for these materials is yttrium iron garnets YIG's in the form  $Y_3Fe_5O_{12}$ .

### **2. According to applications**

Ferrimagnetic materials have become available as practical magnetic materials and have a number of important scientific and technological applications. This may be attributed to (Tayal, 1998)

- a. They have relativity large saturation magnetization.
- b. Their resistivities ranged between  $10^2 \Omega.cm$  to  $10^{13} \Omega.cm$  .
- c. They are poor conductors of the electricity, specially, at room temperature.

These properties are valuable in the high frequency application, where the eddy current in the conducting materials poses problems. Ferrimagnetic materials are divided into four groups for applications, which are described in (Dawoud, 1997) as:

#### **i. Hard Ferrites (Permanent Magnets)**

Materials used for this application are barium ferrite  $BaFe_{12}O_{19}$  and strontium ferrite  $SrFe_{12}O_{19}$ . These are hexagonal ferrite with a crystal structure of magneto-plumbite  $PbFe_{12}O_{19}$ . These materials are characterized by a high value of the uniaxial anisotropy field and a high coercive force. In addition, their resistivity is high, typically

$10^8 \Omega \cdot cm$ . The high coercive force allows these materials to be used as focusing magnets for television tubes, where there are strong demagnetization field. The high resistivity permits their use as permanent magnets where there is additional high frequency magnetic flux without eddy current losses (Smit and Wijn, 1959; Snelling, 1964).

## **ii. Soft Ferrites**

Soft ferrites are ferrimagnetic materials with cubic crystal structure and they are characterized by chemical formula  $MO \cdot Fe_2O_3$ , where M is transition metal ions like Iron, Nickel, Manganese or Zinc.

The essential requirement is materials with high permeability, low coercive force, low eddy current losses and the ability to operate up to frequencies of 10 MHz with special requirements extending to 1000 MHz. The initial permeability of the manganese and the nickel ferrite is rather low, about  $250 (H \cdot m^{-1})$  and  $10 (H \cdot m^{-1})$ , respectively. If these materials are combined with zinc, the anisotropy is lowered and the permeability increases to about  $1000 (H \cdot m^{-1})$  for the mixed *Mn-Zn* ferrite and  $700 (H \cdot m^{-1})$  for the mixed *Ni-Zn* ferrite. The latter has the higher resistivity and lower losses with higher permeability (Snelling, 1969).

## **iii. Rectangular Loop Ferrites**

Rectangular Loop Ferrites are ferrites which have a rectangular hysteresis loop. This property makes them suitable for use in a magnetic memory core. Ferrite communities used for this application are the mixed *Mn-Mg* ferrite and the mixed *Li-Ni* ferrite (Albers, 1954; Peloschek, 1963).

## **iv. Microwave Ferrites**

The processing of electromagnetic waves which is done in the frequency range from 1 GHz to 100 GHz are applications of Microwave Ferrites. This processing depends on the interaction of the electromagnetic waves with the processing spin moments in the ferrites. The discussion is restricted to one of the most important of those processes known as Faraday rotation. This is the rotation of the plane of polarization of a plane electromagnetic wave as it travels through the ferrites in the direction of the applied magnetic field. The most application of the Faraday rotation is to use waveguide just as

one uses polarizer and analyser in optics to accept or reject plane polarized wave. The most important microwave ferrites are manganese ferrite, nickel ferrite, cobalt ferrite and the mixed *Ni-Mn* ferrite (Lax and Button, 1962).

### **Aim of this Study**

The aim of this study is to investigate the effect of nickel ions on the magnetic, electric and dielectric properties of mixed *Li-Ni* spinel ferrite. AC circuits are used to study the above properties for the mixed *Li-Ni* spinel ferrite which was prepared by standard double sintering ceramic technique and have chemical formula of ( $Li_{0.5(1-x)}Ni_xFe_{2.5-0.5x}O_4$ ) where  $x$  is the percentage of  $Ni^{2+}$  ions in the compound which changes in steps of  $0.2$  according to  $0.0 \leq x \leq 1.0$ .

# **CHAPTER 1**

## **Theoretical Background**

# CHAPTER 1

## Theoretical Background

Ferrites are magnetic oxide materials with semiconducting nature, which are of great technological importance by virtue of their interesting electrical and magnetic properties, so it is important to introduce a theoretical preview about structure, magnetic, electric and dielectric properties of ferrites, which includes in this chapter.

### 1.1 Structure of Spinel Ferrite Materials

Ferrimagnetic spinel ferrites are the most common compound of the ferrimagnetic materials. The concept of the simplest structure of the ferrimagnetic spinel materials includes two magnetic sublattices. The structure of the ferrite affects the physical properties of these ferrite materials.

#### 1.1.1 Spinel Lattice Structure

The term ferrite denotes a group of iron oxides which have the general formula " $MO \cdot Fe_2O_3$ ", where  $M$  is a divalent metal ion such as  $Mn^{2+}$ ,  $Fe^{2+}$ ,  $Co^{2+}$ ,  $Ni^{2+}$ ,  $Cu^{2+}$ ,  $Zn^{2+}$ ,  $Mg^{2+}$  or  $cd^{2+}$ . Magnetite  $Fe_3O_4$  (or  $FeO \cdot Fe_2O_3$ ) is a typical ferrite which has been a well-known magnetic oxide since ancient times. By replacing the divalent iron in  $Fe_3O_4$  by another divalent ion, ferrites can be produced which have different intensities, of intrinsic magnetization. Furthermore, just as we can get various magnetic alloys by mixing a number of metal elements, by mixing two or more kinds of  $M^{2+}$  ions we can obtain mixed ferrites, which show various interesting and useful magnetic properties As shown in figure (1.2),  $A$  ions fill the tetrahedral interstices, i.e.  $T_d$  sites, and  $B$  ions fill the octahedral interstices, i.e.  $O_h$  sites, of the cations packing (Gorter, 1954). The lattice constant "a" for these materials varies with the compositions, it is about  $8.5 \text{ \AA}$ . Figure (1.3) shows an isolated  $O^{2-}$  ion with its nearest neighbours of the  $A$  and  $B$  ions (Dawoud, 1997). Oxygen atoms have an ionic radius of about  $1.32 \text{ \AA}$ , this is larger than the ionic radius of the metal ions, which varies between  $0.6 \text{ \AA}$  to  $0.8 \text{ \AA}$  (Chikazumi, 1964). Spinel lattice distribution is affected by many factors like electrons configuration, electrostatic energy and ionic radii, this tends that, the metal ions occupy the interstitial

position sites of the spinel lattice structure, which can be classified into two groups (Dawoud, 1997)

- i. The  $T_d$  sites interstices are filled by the  $A$  ions, which have the ionic charge  $p$  and surround by four  $O^{2-}$  ions. They are represented by the bracket ( ).
- ii. The  $O_h$  sites interstices are filled by the  $B$  ions, which have the ionic charge  $q$  and surround by six  $O^{2-}$  ions. They are represented by the bracket { }.

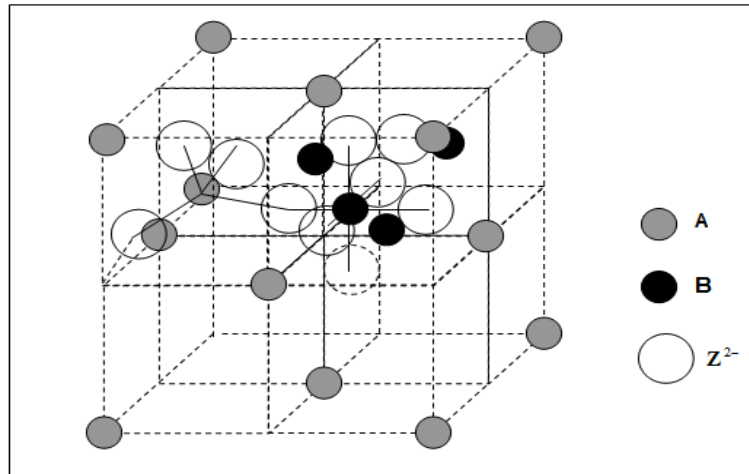


**Figure (1.2):** Two octants of the unit cell of the spinel lattice structure  $A$  ions are at  $T_d$  sites and  $B$  ions are at  $O_h$  sites of the  $Z^{2-}$  anions packing.

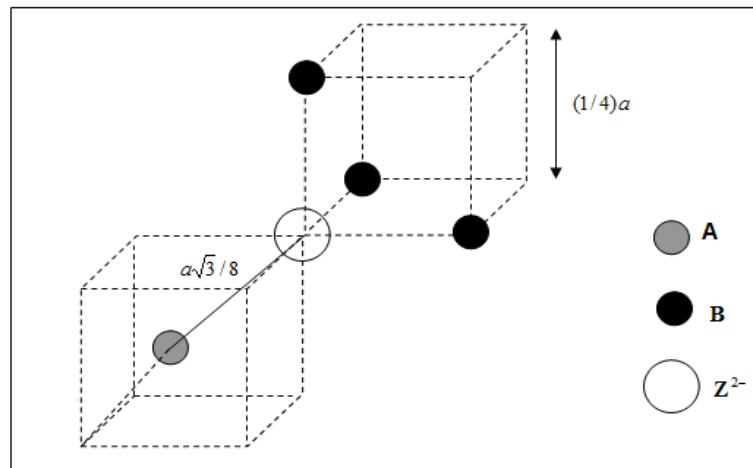


**Figure (1.3):** An anion  $Z^{2-}$  in the spinel lattice structure with its nearest cations neighbours.

In the spinel lattice structure, the anions have a negative charge equal (-8), which comes from the four  $O^{2-}$  ions. Therefore, the total sum of the ionic charge of the cations, i.e.  $p$  and  $q$ , should be equal (+8). There are various possibilities of the ionic charge distribution of the cations of the spinel lattice structure which depend on the  $A$  and the  $B$  ions, while the cubic closed- packed lattice of the material is the same. The various possibilities of  $p$  and  $q$  values were listed in Table (1.1) (Verwey and Helimann, 1947).

**Table (1.1):** Various possibilities of the ionic charge distribution of the cations of the spinel lattice structure.

Ionic charge value		Ionic Charge Distribution of Spinel Lattice	Type of Spinel Materials
P	q		
2	3	$(A_1^{2+})\{B_2^{3+}\}Z_4^{2-}$	(2-3) Spinel Type.
4	2	$(A_1^{4+})\{B_2^{2+}\}Z_4^{2-}$	(4-2) Spinel Type.
3	5/2	$(A_1^{3+})\{B_2^{(5/2)+}\}Z_4^{2-}$	(3-5/2) Spinel Type.
6	1	$(A_1^{6+})\{B_2^{1+}\}Z_4^{2-}$	(6-1) Spinel Type.

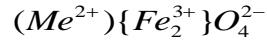
The common type of the spinel lattice structure is (2-3) spinel type, which have the highest electrostatic stability in the normal cations arrangement (Verwey, Deboer and Vansanten, 1948). Hence, the  $A$  and the  $B$  ions have various distributions, this makes a change in some of the physical properties of these materials. The simplest example for the ferrimagnetic spinel materials are the spinel iron, e.g. magnetite (magnetic oxide of iron) in the form  $(Fe_1^{2+}Fe_2^{3+}O_4^{2-})$ . Several mixed spinel ferrites can be produced by adding different oxides to the iron oxides, which give useful physical properties for several applications.

### 1.1.2 Types of Spinel Lattice Structure

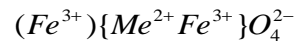
The distribution of the metal ions at  $T_d$  and  $O_h$  sites is very important to understand the physical properties of the ferrimagnetic materials. More than one type of this distribution is found at the two sites for the materials in the form  $MeFe_2O_4$ .

These types are described by (Dawoud, 1997) as:

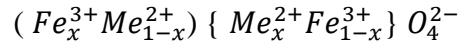
**i. Normal Spinel Structure:** In this type, all the  $Me^{2+}$  divalent metal ions are found on the  $T_d$  sites and the  $Fe^{3+}$  trivalent iron ions appear only on the  $O_h$  sites. The formula of this type is found in the form



**ii. Inverse Spinel Structure:** In this type, all the  $Me^{2+}$  divalent metal ions are found on the  $O_h$  sites and  $Fe^{3+}$  trivalent iron ions are distributed in equal numbers over  $T_d$  and  $O_h$  sites. The formula of this type is found in the form



**iii. Intermediate Spinel Structure:** In the intermediate spinel structure the divalent metal ions  $Me^{2+}$  and the trivalent iron ions  $Fe^{3+}$  are distributed on the  $T_d$  and  $O_h$  sites. The formula of this type is found in the form



### 1.1.3 The Factors Affecting on the Structure

There are some factors which can be influence the distribution of the metal ions over the  $T_d$  and  $O_h$  -sites. These factors are:

#### **i. The Ionic Radius:**

According to the oxygen distribution we can evaluate that  $T_d$  -site is smaller than  $O_h$  -site. So, one might expect that the smaller ions will prefer to occupy the tetrahedral sites. Trivalent ions are usually smaller than divalent ions, and this tends to favor the inverse structure.

#### **ii. The Electronic Configuration:**

Certain ions have a special preference for a certain environment, e.g.,  $Zn^{2+}$  ( $4s^2 3d^{10}$ ) and  $cd^{2+}$  ( $5s^2 4d^{10}$ ) preferences for  $T_d$  -sites where their electrons can form a covalent bond with the six 2P electrons of the oxygen ions.



### iii. Electrostatic Energy or "Madelung" energy of the spinel lattice:

This is the electrostatic energy gained when the ions, at first thought to be infinitely far apart, are brought together to form the spinel lattice. In the normal arrangement the metal ions with smallest (+ ve) charge are surrounded by 4 oxygen ions, and the metal ions, which is electrostatically most favorable.

## 1.2 Magnetic Properties of the Ferrimagnetic Materials

The ferrites are ionic compounds, and their magnetic properties are due to the magnetic ions they contain. Since it is difficult to calculate the orbital magnetic moments in the ionic crystal, the intensity of the intrinsic magnetization of the ferrimagnetic spinel materials can be explained according to the spins distribution of the magnetic ions at the  $T_d$  sites and the magnetic ions at the  $O_h$  sites that shown in figure (1.4) (Dawoud, 1997; Lovell, Avery and Vernon, 1976) . It arises usually from the spin magnetic moments of the unfilled shells 3d, for the transition elements, where the superexchange interaction between the sublattices and the six-2p oxygen electrons occurred. Such that an alignment of spins should be expected from the nature of the superexchange interactions. The superexchange interactions between the two cations; via an intermediate  $O^{2+}$  ions are greatest, if the three ions are collinear and their separations are not too large.

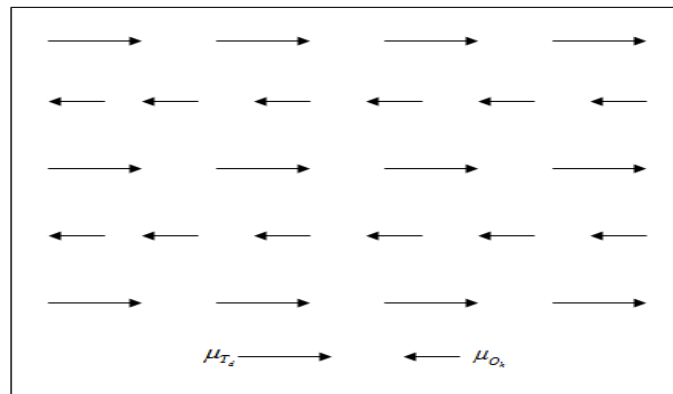


**Figure (1.4):** Spins distribution at  $T_d$  and  $O_h$  sites.

The ions arrangement in the spinel lattice is likely to be most important as is shown in figure (1.5 a through e) (Morrish, 1965; Smit and Wijn, 1959). For the situation depicted

in figure (1.5) both the angle  $\varphi$  and the distance between the ion cores are favorable for superexchange interactions. For all the other cases, either the angle of figure (1.5 c) or the distance of figures (1.5 b and 1.5 d), or both figure (1.5 e) are unfavorable. The conclusion is that the interactions between the sublattices are stronger than those within them. Further, these interactions between the ions within the  $T_d$  sites are the weakest of all. This result thus, supports the assumption that the sublattices magnetizations are antiparallel.

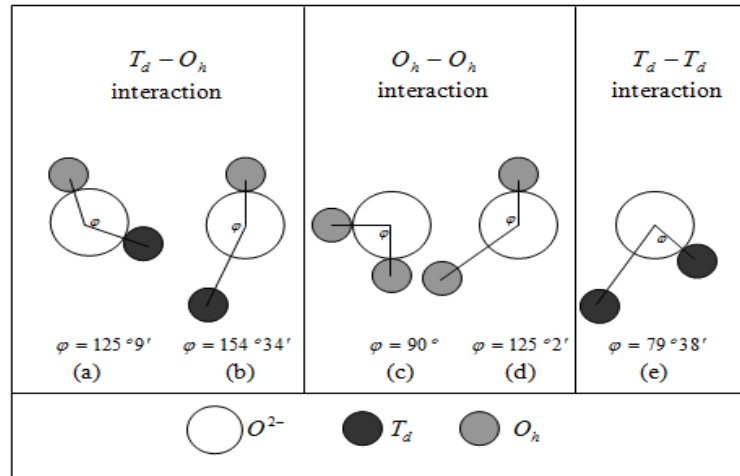


**Figure (1.5):** Super exchange interactions between the anions,  $O^{2-}$  ions, and the cations, the  $T_d$  and the  $O_h$  sites.

### 1.2.1 Magnetization Process of the Ferrimagnetic Materials

The relation between the flux density,  $B$  ( $wb.m^{-2}$ ), and the applied field intensity,  $H$  ( $A.m^{-1}$ ), is not linear for ferrimagnetic materials. It depends on the previous magnetic history, mechanical and thermal properties as well as on the treatment of the materials being tested. When  $H$  is applied to the ferrimagnetic substance, the resulting  $B$  is composed of the free space and the contribution of the aligned domains. The  $B$  can be expressed as following (Crangle, 1991)

$$B = \mu_0 (H + M) \quad (1.1)$$

where

$$\mu_0 = 4\pi \times 10^{-7} \text{ (wb.m/A) is the permeability of the free space.}$$

$H$  ( $A.m^{-1}$ ) is the applied magnetic field intensity.

$M$  ( $A.m^{-1}$ ) is the intensity of the intrinsic magnetization of the substance.

Equation (1.1) is exact for all substances including ferrimagnetic materials. It is useful to define  $M$  by

$$M = \chi_m H \quad (1.2)$$

where  $\chi_m$  is a dimensionless quantity which is known as the magnetic susceptibility of the material. Substituting equation (1.2) into equation (1.1), this gives

$$\begin{aligned} B &= \mu_o (1 + \chi_m) H \\ B &= \mu_o \mu_r H = \mu H \end{aligned} \quad (1.3)$$

where  $\mu_r = 1 + \chi_m$  is a new dimensionless quantity which is known the relative permeability and  $\mu$  ( $\mu = \mu_o \mu_r$ ) is the permeability of the substance.

### 1.2.2 Ferrimagnetic Domains

All ferrimagnetic materials consist of many microscopic regions called Weiss domains (Ferroxcube, 2002), within them all the magnetic moments are aligned in the same direction. These domains have a volume of about  $10^{-12} m^3$  to  $10^{-8} m^3$  and contain  $10^{17}$  to  $10^{21}$  atoms (Serway, 1996). The magnetizations within the domains are called the intrinsic magnetization per unit mass at temperature  $T$  and its value at zero  $H$  is the spontaneous magnetization. The saturation magnetization ( $M_s$ ) is the value of the spontaneous magnetization at zero temperature (Crangle, 1991).

In unmagnetized sample of the ferrimagnetic substance, the domains are randomly oriented; therefore,  $\mu_{net}$  is zero. As shown in figure (1.6 a), the domains are randomly oriented since there is no external magnetic field applied to the unmagnetized sample. When  $H$  increases, the domains become more aligned in the direction of  $H$  by rotating slightly until all of them are nearly aligned as shown in figure (1.6 d). At this state, the saturation condition corresponds to the state where all domains are in the same direction parallel to  $H$ , which results in a magnetized sample (Ferroxcube, 2002).

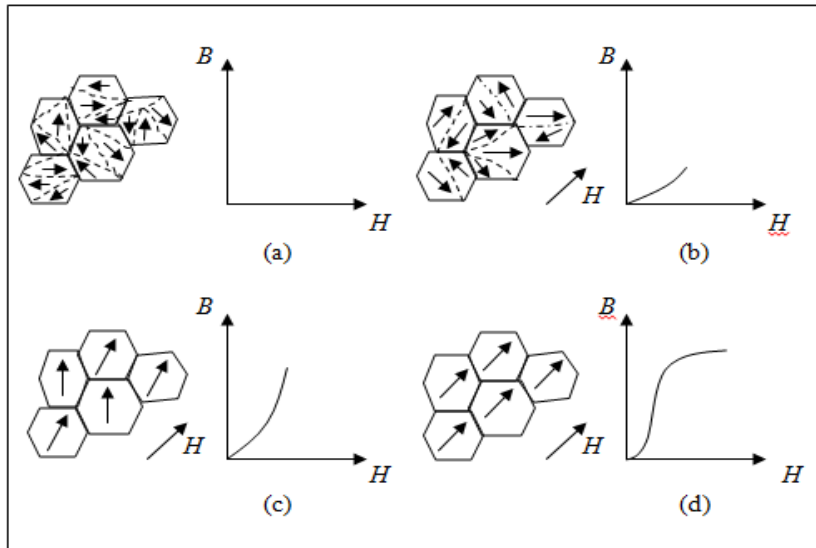


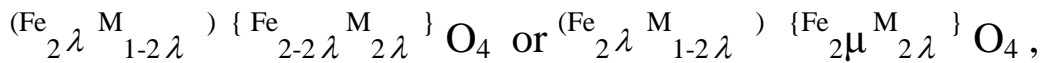
**Figure (1.6):** Alignment of Weiss domains.

### 1.2.3 Molecular Field Theory of the Ferrimagnetic Materials

Neel (Neel, 1948) considered that, a ferrimagnetic crystal lattice could be divided into two magnetic sublattices or groups, i.e.  $T_d$  and  $O_h$  sites, in the spinel lattice structure, where their magnetic moments are not equal, so that, a net magnetic moment is found. He supposed the existence in the material of one type of magnetic ion only, of which a fraction  $\lambda$  appeared on  $T_d$  sites and a fraction  $\mu$  on  $O_h$  sites. Thus

$$\lambda + \mu = 1$$

The remaining occupied lattice sites were assumed to house only ions of zero magnetic moment. Considering a simple ferrite of the form  $MFe_2O_4$ , which satisfies Neel's assumptions, the magnetic ions are trivalent ferric  $Fe^{3+}$ . M is non-magnetic and the formula might be written,



where the  $T_d$  sites are represented by the bracket ( ) and  $O_h$  sites { }.

Since an ion on  $T_d$  has near neighbors both  $T_d$  and  $O_h$ -sites, as has an ion on  $O_h$ -sites, there are several interaction between magnetic ions to be considered and these may be classed as  $-T_d-T_d$ ,  $O_h-O_h$ ,  $T_d-O_h$ , and  $O_h-T_d$  (where  $T_d-T_d$  refers to the

interaction of an ion on an  $T_d$  sites with its neighbors also on  $T_d$  sites, with similar definitions for the other term). In the Neel theory it is assumed that the  $T_d - O_h$  and  $O_h - T_d$  interactions are identical and predominate over  $T_d - T_d$  and  $O_h - O_h$  interactions, and are such as to favor the alignment of the magnetic moment of each A-ion more or less antiparallel with the moment of each B-ion. Thus for the ferrites considered above, assuming each ferric ion to have a moment of 5 Bohr magneton ( $\mu_B$ ), the moment of the ferrite "molecule" would be  $2(\lambda - \mu) 5 \mu_B$  instead of  $2(\lambda + \mu) 5 \mu_B$ , which would occur with parallel orientation of all the moments. The Neel theory predicts magnetic moments which may be much smaller than the sum of the moments of the constituent ions. This is experimentally observed. Clearly, Neel's assumption that only one type of magnetic ion is present will rarely be met, but it has been found that the general features of ferrites may be adequately represented on the Neel model, with suitable qualitative modifications.

Neel defined the interactions within the material from the Weiss molecular field view point. The magnetic field acting upon an atom or ion is written in the form

$$H = H_X + H_m, \quad (1.4)$$

where  $H_X$  is the externally applied field and  $H_m$  is the internal or molecular field which arises due to interactions with other atoms or ions within the material.

When the molecular field concept is applied to a Ferrimagnetic material we have

$$H_T = H_{TT} + H_{TO}, H_O = H_{OO} + H_{OT} \quad (1.5)$$

Here the molecular field  $H_T$ , acting on an ion on an  $T_d$ -site, is represented as the sum of the molecular field  $H_{TT}$  due to neighbors on  $T_d$ -sites, and  $H_{TO}$  due to its neighbors on  $O_h$ -sites. A similar definition holds for the molecular field  $H_O$ , acting on an ion on  $O_h$ -sites.

The molecular field components may then be written as

$$H_{TT} = \gamma_{TT} M_T, H_{TO} = \gamma_{TO} M_O \quad (1.6)$$

$$H_{OO} = \gamma_{OO} M_O, H_{OT} = \gamma_{OT} M_T \quad (1.7)$$

where the  $\gamma$ 's are the appropriate molecular field coefficients and  $M_T$  and  $M_O$  are the magnetic moments of the  $T_d$  and  $O_h$  -sites. It may be shown that,

$$\gamma_{TO} = \gamma_{OT} \quad \text{but} \quad \gamma_{TT} \neq \gamma_{OO}$$

Unless the two sublattices are identical. Neel showed that  $\gamma_{TO} < 0$ , favoring antiparallel arrangements of  $M_T$  and  $M_O$ , gives arises to ferrimagnetism.

It is the convenient first to examine the effect of magnetic fields of the form shown in the eqns (1.6) and (1.7) upon the macroscopic magnetic properties of ferrimagnetic in the high temperature ranges where paramagnetic susceptibility values are observed.

In an assembly of  $N$  free paramagnetic ions per unit volume, each with angular momentum quantum number  $J$ , the magnetization is given by (Morrish, 1965) :

$$M = NgJ \mu_B B_J(x) \quad (1.8)$$

where  $B_J(x)$  is the **Brillouin** function, using mathematics and under a certain condition one can get (Zaki, 1992):

$$M = \mu_o N g^2 \mu_B^2 J(J+1) H/3KT \quad (1.9)$$

where  $K$  is the **Boltzmann's** constant and  $T$  is the absolute temperature. Thus the volume susceptibility defined as  $\chi_m = M/H$  is given by

$$\chi_m = \mu_o N g^2 \mu_B^2 J(J+1)/3KT = C/T, \text{ the Curie law.}$$

If the magnetic field in the Curie law is taken to be  $(H_X + H_m)$ . Then we have

$$M/(H + H_m) = M/(H + \gamma M) = C/T \quad (1.10)$$

and this leads to the Curie-Wiess law

$$\chi_m = C/(T - T_C) \quad (1.11)$$

Since  $T_C = \lambda C$ , this affords a method for the experimental determination of the molecular field coefficient.

Writing  $\chi_m = (M/H_X)$  and  $M = M_T + M_O$  it follows after the necessary algebraic manipulation, and following Neel we can get, (Neel, 1948) :

$$\frac{1}{\chi_m} = \frac{T}{C} + \frac{1}{\chi_{mX}} - \frac{\eta}{T - \theta} \quad (1.12)$$

where

$$\frac{1}{\chi_{mX}} = \gamma_{TO} (2\lambda\mu - \lambda^2\alpha - \mu^2\beta),$$

$$\theta = \gamma_{TO} \lambda\mu C (2 + \alpha + \beta),$$

$$\eta = \gamma_{TO}^2 \lambda\mu C [\lambda(1 + \alpha) - \mu(1 + \beta)]^2,$$

$$\alpha = (\gamma_{TT} / \gamma_{TO}) \text{ and } \beta = (\gamma_{OO} / \gamma_{TO})$$

The first two terms on the right hand side of equation (1.12) give the Curie-Weiss form of temperature dependence of  $\frac{1}{\chi_m}$  found in ferromagnetic above the Curie point, but the

final term has no counterpart in the ferromagnetic case.

Equation (1.12) represents a hyperbola, shown diagrammatically in figure (1.7). As would be expected well above the Curie point, ferrimagnetic interactions play little part and the hyperbola is asymptotic to the line

$$\frac{1}{\chi_m} = \frac{T}{C} + \frac{1}{\chi_{mX}} \quad (1.13)$$

Which cuts the temperature axis at  $T_A = -C/\chi_{mX}$ . Neel called this the asymptotic Curie point. The paramagnetic curie point  $T_c$  is found by equating  $\frac{1}{\chi_m}$  to zero and yields ,

(Neel, 1948) :

$$T_c = \frac{\gamma_{TO}C}{2} [\lambda\alpha + \mu\beta + \{(\lambda\alpha - \mu\beta)^2 + 4\lambda\mu\}^{\frac{1}{2}}]. \quad (1.14)$$

Clearly if  $T_c$  is negative, the material remains with paramagnetic values of susceptibility down to the absolute zero of temperature. But, when  $T_c > 0$ ,

$\chi_m$  becomes theoretically infinite at this temperature, below which a spontaneous magnetization of the material appears and remains finite as the applied magnetic field is reduced to zero.

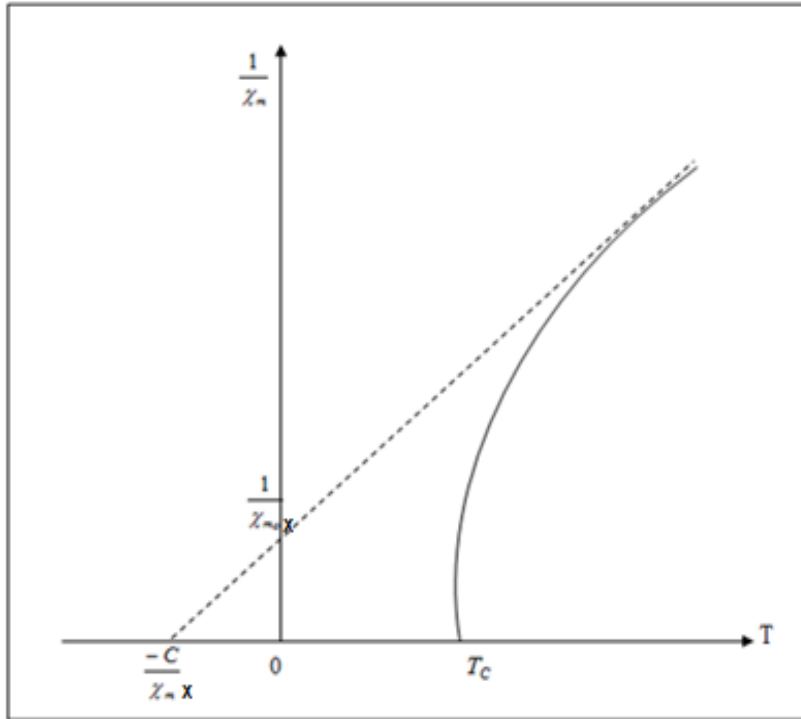


**Figure (1.7):** Inverse magnetic susceptibility of the ferrimagnetic materials above the  $T_C$  according to the molecular field theory.

### 1.3 Electric Properties of the Ferrimagnetic Materials

The electrical properties of ferrites are sensitive to preparation method, sintering temperature, sintering time, rate of heating and rate of cooling (Kulkarni, Todhar and Vaingankar, 1986; Rezlesus and Rezlesus, 1974). The study of electrical conductivity produces valuable information on behavior of free and localized electric charge carried in the sample.

#### 1.3.1 Conductivity of the Ferrimagnetic Materials

The conductivity  $\sigma$  of the ferrimagnetic materials depends on temperature and the measuring frequency of the applied field. This is controlled by the cations concentration on the sites of the spinel lattice structure (Patil, Sawant, Patil and Patil, 1994). Therefore, their conductivity can be expressed according to (Chikazumi, 1964)

$$\sigma = \sigma_o e^{-E_a/kT} \quad (1.15)$$



where  $\sigma_0$  is temperature dependent constant,  $E_a$  represents the activation energy, which is the energy required to release an electron from the ion for a jump to the neighbouring ion, so that, giving rise the electric conductivity, and  $K$  is Boltzmann constant .

Almost all of the known ferrimagnetic materials are poor conductors of electricity, the resistivity  $\rho$  of the ferrites at room temperature varies from  $10^{-2}\Omega.cm$  to  $10^{11}\Omega.cm$ , which depends on the chemical composition (Smit and Wijn, 1959).

### **1.3.2 Conduction Mechanism in the Ferrimagnetic Materials**

The conduction mechanism in the ferrimagnetic materials is different and much less understood in comparison with the elements in-group IV semiconductors such silicon and germanium (Patil et al, 1994).

In the ferrimagnetic materials, the concentration of the charge carriers is larger than semiconductor materials (Verwey, Deboer and Vansanten, 1948). The nature of charge carriers in ferrimagnetic oxides have been the subject of many experimental and theoretical studies, however, until now no conclusive theory has been formulated for conduction mechanism in these materials (Mazen, Ghani and Ashotr, 1985).

The conduction mechanism is attributed to the hopping of the electrons between  $Fe^{2+}$  ions and  $Fe^{3+}$  ions. The  $Fe^{2+}$  ions are considered the donors that contain extra electron, which will jump to the adjacent  $Fe^{3+}$  ions easily and will constitute the electrons conduction. The oxidation of the divalent iron ions reduces donor content in the material such that, the electric resistivity is increased (Cheng, 1984).

The conductivity in ferrites associates with the presence of the ions for the element in more than one valence state; these ions are distributed over the crystallographically inequivalent sites (Patil et al, 1994). The conduction mechanism of the ferrites depends on temperature. Therefore, the conductivity will be described as in equation (1.15).

The detailed behaviour of the complex compounds such that ferrimagnetic materials are not well understood. In general, the conduction at lower temperature is due to hopping electron between  $Fe^{2+} \leftrightarrow Fe^{3+}$  ions (Uitert, 1956), whereas at a higher temperature is due to the hopping polarons (Klinger, 1975; Klinger, 1977)

Since the mobile carriers have spin magnetic moments, they are strongly influenced in their motion by the direction of spins on neighbouring sites. And they can polarize the lattice sites. Therefore, the combination of the mobile carriers and lattice polarization is known as a magnetic polaron (Lovell, Avery and Vernon, 1976).

It is found that, the neighbouring spins forming a "magnetic polaron". However, the motion of the polaron is always characterized by a large effective mass and low mobility. If the polarization is much localized the polaron is called small polaron and usually moves by thermal activation. At high temperatures, the electron moves from site to site by thermally activated hopping; at low temperature the electron tunnels slowly through the crystal (Kittel, 1976). In the neighbourhood of  $T_C$  thermal vibrations are disordering spins. The motion of a charge carrier may be strongly influenced by the scattering produced by the disordered spins.

#### **1.4 Dielectric Properties of the Ferrimagnetic Materials**

The polycrystalline ferrites, which have many applications at microwave frequencies are very good dielectric materials. The dielectric properties of the ferrites depend on several factors including (Ravinder and Latha, 1999) the method of preparation, sintering temperature, sintering atmosphere, frequency applied and chemical composition.

When a ferrite powder is sintered under gradually reducing conditions the divalent iron ions are formed in the bulk. This leads to high conductivity ferrite grains, which has a very high dielectric constant  $\epsilon$  (Eatah, Ghani and Faramawy, 1988). The electrons exchange interaction between the  $Fe^{2+}$  ions and the  $Fe^{3+}$  ions result in a local displacement of the electrons in the direction of the electric field. This determines the polarization of the ferrites. Therefore, the  $Fe^{2+}$  ions play a dominant role in the mechanisms of the conductivity and the electric polarization. The concentration of the  $Fe^{2+}$  ions depends on sintering temperature and sintering atmosphere (Reddy and Reddy, 1991).

In order to obtain quantitative information about the behaviour of the ferrite, precise impedance measurements were carried out with disks of several compositions. In general, the dielectric constant is roughly inversely proportional to the square root of the resistivity. Both quantities depend on the measuring frequency of the applied field (Smit and Wijn, 1959).

# **CHAPTER 2**

## **Literature Survey**

## CHAPTER 2

### Literature Survey

This chapter contains some of the previous studies for various ferrite systems which have the same trend of the subject of the mixed *Li-Ni* spinel ferrite. Some of these studies have illustrated the magnetic, the electric and the dielectric properties for different ferrite systems.

#### 2.1 Magnetic Properties

**Venkataraju et al**, (Venkataraju ,Sathishkumar and Sivakumar, 2010), studied Nanoparticles of  $Mn_{(0.5-x)}Ni_xZn_{0.5}Fe_2O_4$  ( $x= 0.0, 0.1, 0.2 , .0.3$  ), it has been synthesized by chemical co- precipitation method . Magnetization decreases with increasing Ni concentration except for  $x=0.3$ , where it shows increasing trend. This is due to migration of  $Fe^{3+}$  ions from B – site to A – site , which reduces the B – B coupling and there by the spin in the B sublattice . The Curie temperature was found to decrease with increase in nickel concentration except for  $x=0.3$ , where it shows arise.

**Sattar et al**, (Sattar, El-Sayed and Agami, 2007), studied the effect of Ca substitution on the physical and magnetic properties of  $Li_{0.3-0.5x}Zn_{0.4}Ca_xFe_{2.3-0.5x}O_4$  ferrites ( $x=0.0, 0.01 ,0.02,0.03$  and  $0 .05$ ) prepared by the standard ceramic method. It is found that the saturation magnetization increases up to  $x= 0.01$  and then it decreases. On the other hand, the initial permeability decreased while the Curie temperature remained almost constant with increasing  $x$ .

**Jadhav**, (Jadhav,2001), studied the magnetic properties for the  $Zn^{2+}$  ions substituted on the mixed *Li-Cu* ferrite in the form  $Li_sCu_{0.4}Zn_{0.6-2s}Fe_{2+s}O_4$ . He showed that, the magnetization increased with increasing of the  $Zn^{2+}$  ions until it reached the maximum value for  $s = 0.3$ , then it decreased by adding the  $Zn^{2+}$  ions. He noticed that, the initial permeability increased slowly with increasing of temperature till reach a

maximum value and then it sharply dropped to zero at **Curie** temperature point, which decreased continuously with increasing of the  $Zn^{2+}$  ions.

## 2.2 Electric Properties

**Dawoud et al,**( Dawoud, A- Ouda and Shaat ,2017), studied the electric properties of the mixed polycrystalline ferrites  $Zn_{1-s}Ni_sFe_2O_4$  , the AC electrical conductivity ( $\sigma_{AC}$ ) over a variable angular frequency in range of  $[(6 - 628) \times 10^4(rad.s^{-1})]$  at room temperature.  $\sigma_{AC}$  shows a continuous increasing with the increasing of the applied angular frequency.

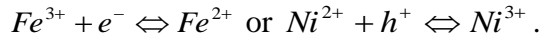
**Nilima et al,** (Nilima, Maisnam and Phanjoubam, 2015), studied the electric properties of the Li-Ni ferrite With the formula of  $Li_{(0.45-0.5x)}Ni_{0.1}Co_xFe_{(2.45-0.5x)}O_4$  prepared by the chemical sol- gel method . The studied of the frequency variation of A.C. conductivity found to increase with the increase of frequency. The substitution of  $Co^{2+}$  plays significant role in influencing the various structural and electrical properties .

**Venkataraju et al,** (Venkataraju et al, 2010), Studied the electrical properties of nanoparticles of  $Mn_{(0.5-x)}Ni_xZn_{0.5}Fe_2O_4$ (  $x= 0.0, 0.1, 0.2 , .0.3$  and 0.5) have been synthesized by chemical co- precipitation method. The resistivity was found to increase with increase in Ni concentration and decrease with increase in temperature.

## 2.3 Dielectric properties

**Dawoud et al,**( Dawoud et al, 2017), studied the *Dielectric Properties* of the mixed polycrystalline ferrites  $Zn_{1-s}Ni_sFe_2O_4$ , for different concentration of Ni content. Double probe electrode method was used to measure the real dielectric constant ( $\epsilon'$ ), the imaginary dielectric constant ( $\epsilon''$ ) and the dielectric loss tangent ( $\tan \delta$ ) over a variable angular frequency in range of  $[(6 - 628) \times 10^4(rad.s^{-1})]$  at room temperature. The results obtained from the dielectric parameter for all the samples decreases with increasing of frequency, which indicated to normal spinel ferrite behavior. The variation

of AC conductivity and dielectric parameters were explained on the basis of electronic exchange between



**Aravind et al**, (Aravind, Raghasudha and Ravinder, 2015), studied the dielectric properties for the Nano crystalline spinel ferrites having compositional formula  $Li_{0.5-0.5x}Ni_xFe_{2.5-0.5x}O_4$  (where  $x = (0.0 \text{ to } 1.0 \text{ with step of } 0.2)$ ) have been prepared by non-conventional low temperature citrate gel auto combustion method. The dielectric parameters like dielectric constant, dielectric loss tangent ( $\tan\delta$ ) and AC conductivity of the prepared samples were measured by using Agilent E4980A precession LCR meter at room temperature in the frequency range 20-2MHz. The dielectric constant( $\epsilon$ ), dielectric loss tangent ( $\tan \delta$ ) and AC conductivity of the prepared samples shows a normal dielectric behavior of ferrites with frequency which indicates the dielectric dispersion is due to hopping of electrons between the  $Fe^{2+}$  and  $Fe^{3+}$  ions.

**Pathan and Shaikh**, (Pathan and Shaikh, 2012), studied the dielectric properties for the mixed ferrites of  $Li_{0.5} Ni_{(0.25-0.5x)} Co_{0.5x} Zn_{0.5}Fe_2O_4$  (where  $x=0, 0.1, 0.2, 0.3, 0.4$  and  $0.5$ ), were prepared using auto combustion method. The dielectric parameters measured at room temperature in the frequency range 20Hz – 1MHz using a HP4284 impedance analyzer. Plots of dielectric constant ( $\epsilon$ ) vs frequency show normal dielectric behavior of spinel ferrites. The frequency dependence of dielectric loss tangent ( $\tan \delta$ ) is found to display a peak at certain frequency. The composition and frequency dependence of the dielectric constant and dielectric loss tangent is explained in terms of ferrous ion concentration.

# **CHAPTER 3**

## **Experimental Techniques**



## CHAPTER 3

### Experimental Techniques

In this chapter, the experimental techniques will be explained. It includes a description of the preparation method of the ferrite samples "Oxide Method". The method of measuring the induction as a function of temperature and the magnetization as a function of a magnetizing field will also be described. In addition, The apparatus and the electric circuits that used will be illustrated in this chapter.

#### 3.1 Preparation of Samples

The mixed *Li-Ni* ferrite samples in the form  $[Li_{0.5(1-x)}Ni_xFe_{2.5-0.5x}O_4]$ , where *x* is the percentage increment of  $Ni^{2+}$  ions in the compound which changes in a step of 0.2 according to  $0.0 \leq x \leq 1.0$ . It prepared using the standard double sintering ceramic technique by mixing pure metal oxides according to the following solid state reaction

$$0.25(1-x)Li_2CO_3 + xNiO + (1.25 - 0.25x)Fe_2O_3 \rightarrow Li_{0.5(1-x)}Ni_xFe_{2.5-0.5x}O_4 + 0.25(1-x)CO_2$$

Pure metal oxides with purity of 99.99% were used for the preparation of the investigated polycrystalline ferrite samples. Table (3-1) shows the weight of each metal oxide.

**Table (3.1):** Weight of each oxide used to prepare the various samples for the mixed *i-Ni* spinel ferrite.

x	The Result Composition	M.Wt. of $Li_2CO_3$ (gm)	M.Wt. of $NiO$ (gm)	M.Wt. of $Fe_2O_3$ (gm)
0.0	$Li_{0.5}Fe_{2.5}O_4$	1.7841	0.00	19.2785
0.2	$Li_{0.4}Ni_{0.2}Fe_{2.4}O_4$	1.3906	1.4057	18.0319
0.4	$Li_{0.3}Ni_{0.4}Fe_{2.3}O_4$	1.0168	2.741	16.8478
0.6	$Li_{0.2}Ni_{0.6}Fe_{2.2}O_4$	.6613	4.011	15.7215
0.8	$Li_{0.1}Ni_{0.8}Fe_{2.1}O_4$	.32278	5.2205	14.6489
1.0	$NiFe_2O_4$	0.00	6.3736	13.6264

The compositions were weighted using a sensitive electric balance (Strtorius AG Gottingen model BA1105) with accuracy of  $10^{-4} gm$ . Twenty grams of the metal oxides for each preparation of each sample were prepared.

The weighted metal oxides were mixed then grounded to a very fine powder for 5 hours. The mixed powder of the metal oxides were presintered at  $750^{\circ}C$  for soaking time of 3 hours using Muffle Furnace (BIFATHERM model A C62) .

Then The prefired powder was well grounded for 3 hours, then samples were pressed with hydraulic press under constant pressure of  $3 \times 10^8 pa$  . Some samples were pressed in the form of a disc shape which have a diameter  $10.4mm$  with thickness  $t$  (3-5)mm, but others in the form of a toroidal shape which have an outer radius  $r_o$  of  $8.24mm$  and inner radius  $r_i$  of  $3.98mm$  with thickness  $t$  (3-5)mm.

All samples were sintered at  $1000^{\circ}C$  for soaking time of 20 hours using a Muffle Furnaces (BIFATHERM model A C62). After sintering, the samples were left to cool to room temperature over the night. After cooling, the disc samples were polished to obtain the form of circular discs with two uniform parallel surfaces which may be suitable to find the AC electric conductivity, the dielectric constant and the dielectric loss tangent. The toroidal samples were polished to obtain a uniform shape to be suitable to find the magnetization properties and to determine Curie point temperature .

### 3.2 Characterization of the Magnetic Properties

The measurement of the magnetization  $M$  is based on **Faraday's** law of the electromagnetic induction, using the toroidal sample as shown in figure (3.1). The toroidal samples of the ferrites materials are especially used as a transformer core in the magnetization measurements. Different parameters can be defined from the figure (3.1), they are

$t$  is the toroidal sample thickness. It was measured by a micrometer with accuracy  $0.01mm$ .

$r_i$  is the inner radius of the toroidal sample.

$r_o$  is the outer radius of the toroidal sample.

$r_m$  is the average radius of the inner and the outer radius of the toroidal

sample i.e.  $r_m = \frac{r_i + r_o}{2}$ .

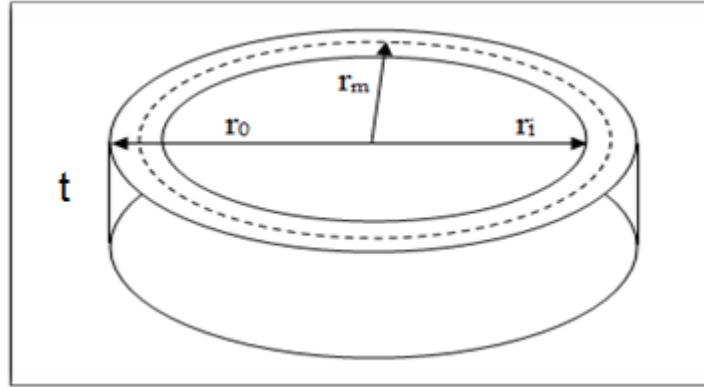


**Figure (3.1):** A toroidal sample shape.

### Magnetization Measurements

The magnetization  $M \text{ A.m}^{-1}$  was determined as a function of the applied magnetizing current passing through the primary coil which changed in the range from (0-5)A at room temperature and frequency  $\nu = 50\text{Hz}$ . The corresponding applied magnetic field  $H \text{ A.m}^{-1}$  varied in the range (200-2650)  $\text{A.m}^{-1}$ , which is calculated by the equation (3.3).

The circuit that has been used in these measurements is shown in the figure (3.2).

The magnetization  $M \text{ A.m}^{-1}$  was calculated from the relation

$$M = \frac{B}{\mu_o} - H \quad (3.1)$$

The scalar quantity of the flux density  $B$  was calculated by (Say M. G., 1976)

$$B = \frac{\sqrt{2}}{N_s \times 50 \times 4.4 \times A} V_s \quad (3.2)$$

where:

$V_s$  is the induced voltage in the secondary coil,

$N_s$  is the number of turns of secondary coil,

$A$  is the cross sectional area of the toroidal sample [ $A=\pi(r_o-r_i)$ ]

One can calculate the corresponding applied magnetic field  $H A.m^{-1}$  using the following relation (Dawoud, 1997)

$$H = \frac{N_p i_p}{2\pi r_m} \quad (3.3)$$

where:

$N_p$  is the number of turns of primary coil

$i_p$  is the current in the primary coil

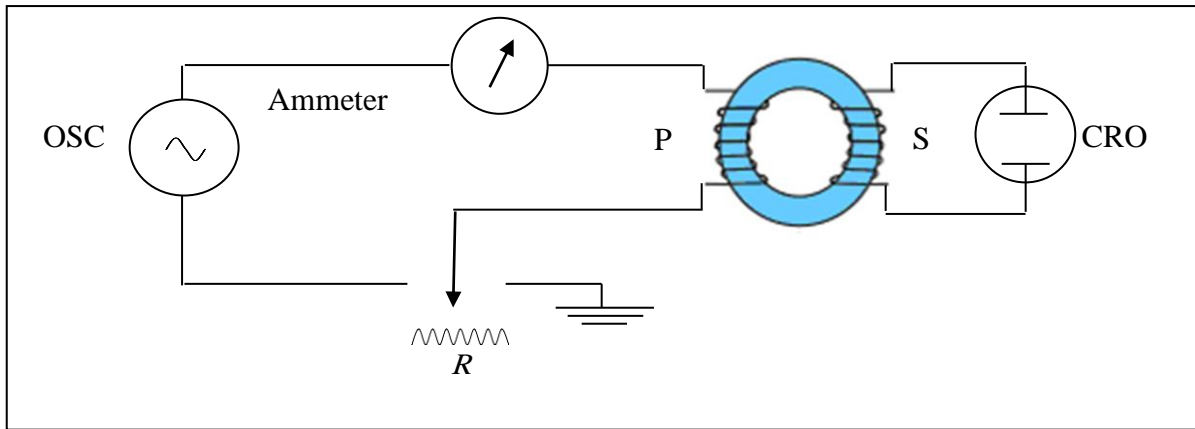


**Figure (3.2):** Circuit diagram for measuring the magnetization using the toroidal samples of the mixed *Li-Ni* spinel ferrite.

### 3.3 Determination of Curie Point Temperature

In order to determine the Curie point temperature, the inductance  $L$  of the toroidal sample is measured as a function of temperature. For inductance measurements, LCR meter model (GW- instek LCR- 821) is used, with series circuit and applied voltage of 1v and constant frequency of 20 KHz with accuracy of ( 0.05% ).

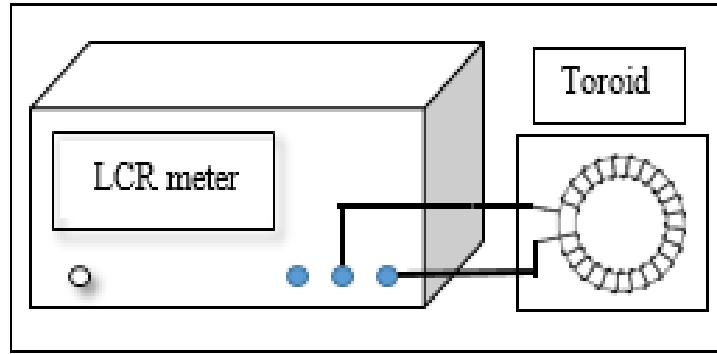


**Figure (3.3):** Circuit diagram for measuring the inductance of the toroidal samples of the mixed *Li-Ni* spinel ferrite.

### 3.4 Characterization of the AC Conductivity and Dielectric Properties

Double probe electrode method was used to measure the AC electrical conductivity, dielectric constant and dielectric loss tangent over a variable range of frequency  $f$  ( $10^4$  Hz up to  $10^6$  Hz) at room temperature. The AC electrical conductivity ( $\sigma_{AC}$ ) was calculated by the relation (Shaht, 2012)

$$\sigma_{AC} = \frac{t}{ZA} \quad (3.4)$$

where  $t$ ,  $Z$  and  $A$  are the thickness, the impedance and the cross-sectional area of a flat surface of the disc samples, respectively.

The permittivity or dielectric constants of the material such as real dielectric constant ( $\epsilon'$ ), the imaginary dielectric constant ( $\epsilon''$ ), the complex dielectric constant ( $\epsilon^*$ ) can be calculated from (Khader et al, 2016)

$$\epsilon' = \frac{C}{C_0} \quad (3.5)$$

where  $C$  and  $C_0$  are the capacitance of the filled and unfilled of the disc sample.

$$\epsilon'' = \frac{\sigma_{AC}}{2\pi f \epsilon_0} \quad (3.6)$$

where  $2\pi f$  is the applied angular frequency and  $\epsilon_0$  is the permittivity of free space.

$$\epsilon^* = \epsilon' - j\epsilon'' \quad (3.7)$$

$$|\epsilon^*| = \sqrt{\epsilon'^2 + \epsilon''^2} \quad (3.8)$$

The dielectric loss tangent ( $\tan \delta$ ) can be determined in terms of real and imaginary parts of dielectric constant as [Shaat, 2012]

$$\tan \delta = \frac{\varepsilon''}{\varepsilon'} \quad (3.9)$$

# **CHAPTER 4**

## **Results and Discussion**

## CHAPTER 4

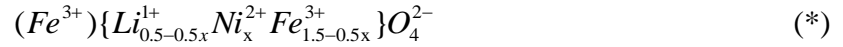
### Results and Discussion

This chapter includes the results and the discussion of magnetic, electric and dielectric properties for the prepared samples of the mixed *Li-Ni* spinel ferrite.

#### 4.1 Magnetic Properties

##### 4.1.1 Magnetic Moment

The net magnetization (M) for the ferrimagnetic materials cannot be observed which is defined by the net magnetic moment ( $\mu_{net}$ ) per unit volume for each sample in **Bohr** magnetons ( $\mu_B$ ) unit. The  $\mu_{net}$  in the unit of  $\mu_B$  was calculated according to the cations distribution that was represented by (\*),



The formula (\*) has a good agreement with the cations distribution, which was suggested by (Sorokhaibam, **Soibam** and **Phanjoubam**, 2015).

According to the formula (\*), the magnetic moment of the  $T_d$  sites ( $\mu_T$ ) and the  $O_h$  sites ( $\mu_O$ ) were calculated using the following equations (Shaah,2004)

$$\mu_T = 2s_{Fe}\mu_B \quad (4.1)$$

$$\mu_O = [xs_{Ni} + (1.5 - .5x)s_{Fe}]2\mu_B \quad (4.2)$$

$$|\vec{\mu}_{net}| = |\vec{\mu}_O| - |\vec{\mu}_T| \quad (4.3)$$

with  $s_{Fe} = 5/2$  and  $s_{Ni} = 1$  are the spin quantum number of the  $Fe^{3+}$  and the  $Ni^{2+}$  ions, respectively, (Dawoud et al , 2017 ). Herein, the  $Li^{1+}$  ions are diamagnetic ions which have no spin quantum number, (A- Mosa , 2016). The variation of the  $\mu_T$ ,  $\mu_O$  and  $\mu_{net}$  with the composition x ( $Ni^{2+}$  ions) are represented in figure (4.1). From this Figure, it can be seen that  $\mu_O$  and  $\mu_{net}$  decreased with increasing of the  $Ni^{2+}$  ions, whereas the  $\mu_T$  stayed constant. The decreasing in the  $\mu_{net}$  with increasing of the  $Ni^{2+}$



ions can be explained by assuming that, with increasing of  $Ni^{2+}$  ions the relative number of the  $Fe^{3+}$  ions decreased in the  $O_h$  sites and fixed in the  $T_d$  sites, which tends to decrease  $\mu_O$ . Therefore, the  $\mu_{net}$  showd linearly decreasing with increasing of the  $Ni^{2+}$  ions.

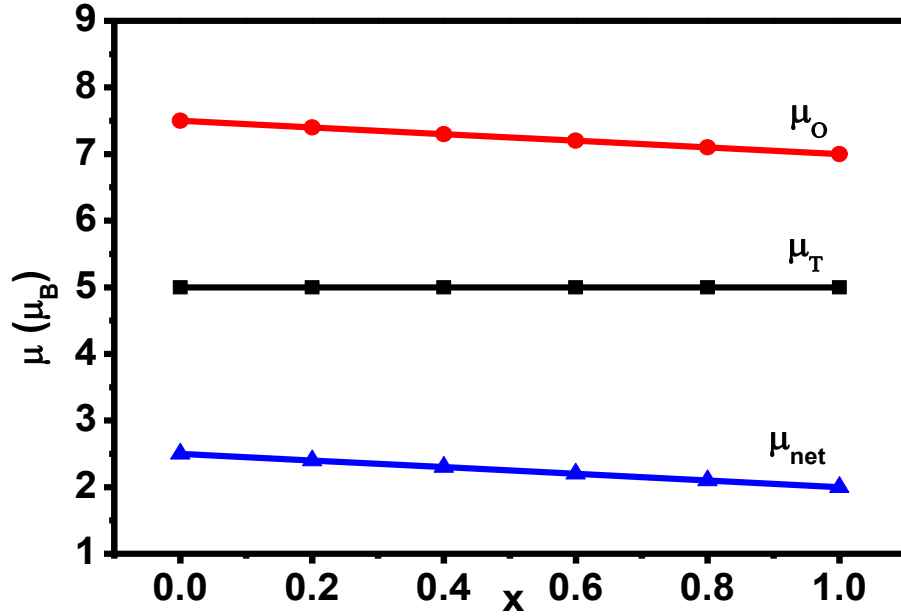


**Figure (4.1):** Variation of  $\mu_O$ ,  $\mu_T$  and  $\mu_{net}$  with the  $Ni^{2+}$  ions concentrations.

#### 4.1.2 Ionic Radii for Tetrahedral and Octahedral Sites

Based on the suggested formula (\*) of the cations distribution for the given mixed Li-Ni spinel ferrites the ionic radius for the  $T_d$  and the  $O_h$  sites can be calculated using the following equations (Potakova, Zverv and Romanov, 1972; Standly, 1972)

$$R_T = R_{Fe^{3+}} \quad (4.4)$$

$$R_O = \frac{1}{2} [xR_{Ni^{2+}} + (0.5 - 0.5x)R_{Li^{1+}} + (1.5 - 0.5x)R_{Fe^{3+}}] \quad (4.5)$$

where  $R_{Ni^{2+}}$ ,  $R_{Fe^{3+}}$  and  $R_{Li^{1+}}$  are the ionic radii of the  $Ni^{2+}$  ion (0.069 nm),  $Fe^{3+}$  ion

(0.064 nm) and  $Li^{1+}$  (0.073 nm), respectively, (Lafta, Al-Shakarchi, Musa, Farle and Salikov, 2015).

In Figure (4.2), the ionic radii  $R_T$  and  $R_O$  are plotted versus the composition  $x$  ( $Ni^{2+}$  ions). As in Figure (4.2), it is clear that, with increasing of the  $Ni^{2+}$  ions the  $R_T$  remain constant while  $R_O$  increased. This behavior is attributed to replacement of the small ionic radius of the  $Fe^{3+}$  ions with the large ionic radius of  $Ni^{2+}$  ions in the  $O_h$  sites.

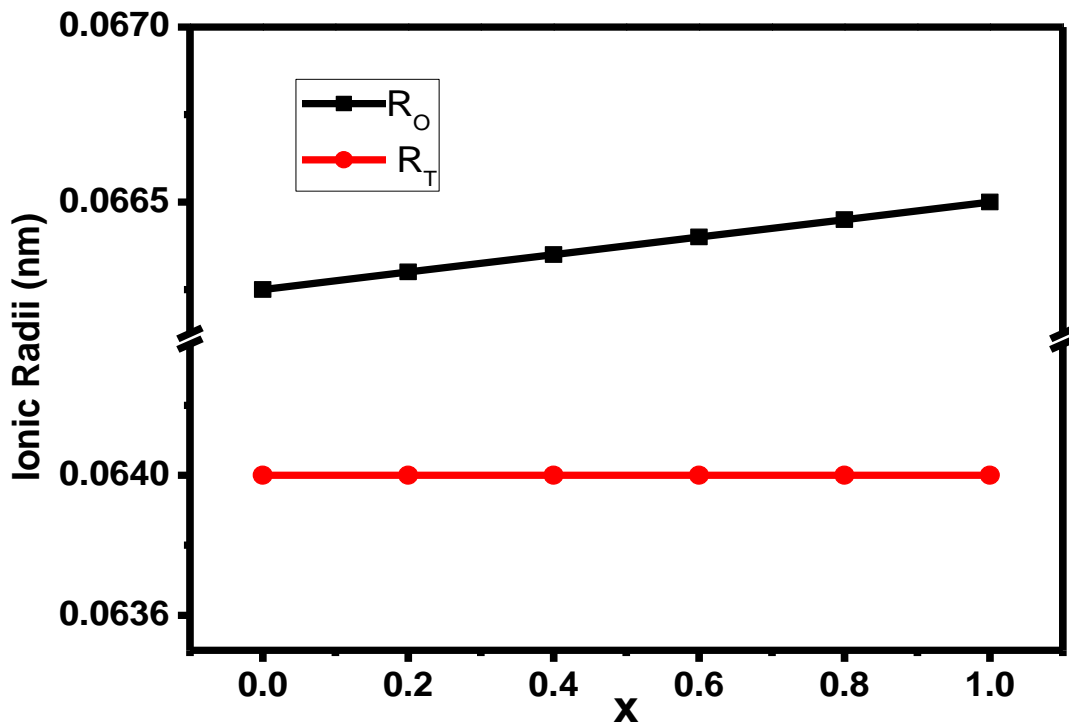


**Figure (4.2):** Variation of  $R_T$  and  $R_O$  with the  $Ni^{2+}$  ions concentrations.

#### 4.1.3 Magnetization Measurement

The magnetic properties for the spinel ferrite can be understood in term of cations distribution and exchange interactions between the two sub lattices,  $T_d$  and  $O_h$  of spinel structure. The relation between the  $M$  ( $A/m$ ) and the applied magnetic field intensity (H) in the range of [200-2650 ( $A/m$ )] for the prepared spinel ferrite samples

of the system  $Li_{.5-.5x}Ni_xFe_{(2.5-.5x)}O_4$  were studied at room temperature of 299 K. The obtained results for the ferrite samples were illustrated in Figure (4.3). From this Figure, it can be seen that  $M$  decreases with increasing of the  $Ni^{2+}$  ions concentration. This behavior can be explained by Neel's two-sublattice model of the magnetism theory of the ferrimagnetic materials (standly, 1972). According to this model, the magnetic ordering in the simple spinel ferrites is based on  $T_d$  and  $O_h$  sites and the resultant magnetization are the difference between two of them provided that they are collinear and anti-parallel to each other. In mixed  $Li-Ni$  spinel ferrite,  $Ni^{2+}$  ions preferentially in  $O_h$  site in the cubic spinel lattice. Therefore, by adding of the  $Ni^{2+}$  ions (low spin quantum number) the concentration of  $Fe^{3+}$  ions (high spin quantum number) in the  $O_h$  site, which implies to decrease the  $M$ . Thus; the decrease of  $M$  is, also, attributed to that  $T_d-O_h$  exchange interaction becomes weaker or comparable with  $O_h-O_h$  exchange interactions.

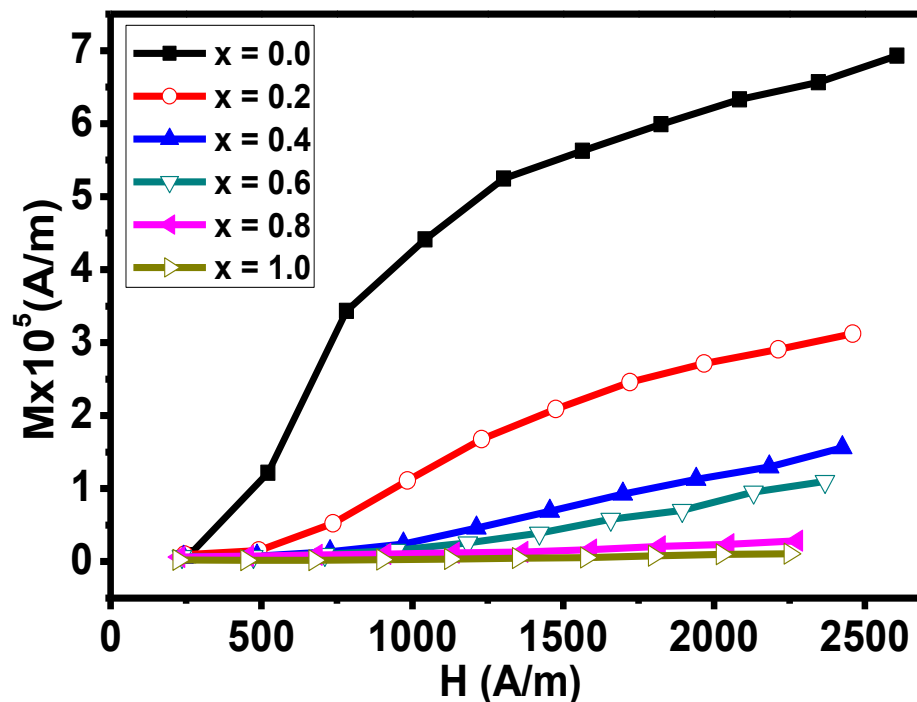


**Figure (4.3):** Variation of  $M$  with  $H$  for the samples with  $x = 0.0, 0.2, 0.4, 0.6, 0.8$  and  $1.0$ .

#### 4.1.4 Relative Permeability

The relative permeability  $\mu_r$  for all samples gives the description of the magnetization behavior during the change of the exposed external applied field. It is defined as the ratio between the induction field ( $B$ ) and the intensity of the  $H$ , i.e.  $\mu_r = B / \mu_o H$  with  $\mu_o$  is the free space permeability. The relation between  $H$  and  $\mu_r$  has an interesting behavior for the present ferrite samples as shown in Figure (4.4). As indicated in this Figure,  $\mu_r$  increased with increasing of the  $H$  and decreasing with the increase of  $Ni^{2+}$  ions. The increment of  $\mu_r$  could be related to the alignment effect of  $H$  on the ionic spins. In such away, the increasing of  $H$  causes rapid increasing of  $B$ , which causing a pronounced increasing of  $\mu_r$ . The behavior of  $\mu_r$  versus  $H$  for samples of  $x=0.0$  was divided into two stages I and II as in Figure (4.4). In stage I,  $\mu_r$  increases with increasing of  $H$  up to  $H = 750$  A/m then  $\mu_r$  decreases. The increasing of  $H$  causes a very rapid increase in  $B$ , which imply to increase  $\mu_r$ . This behavior can be related to the aligning effect of  $H$  on the ionic spins. In stage II,  $\mu_r$  decreasing with increasing of  $H$  might be cause a slight increase of  $B$ , which can be explained as that this sample have the highest spin ordering. This means that, the ionic ordering of this sample is closer to the saturation state. The same behavior was observed by H. Dawoud (Dawoud, 1997).

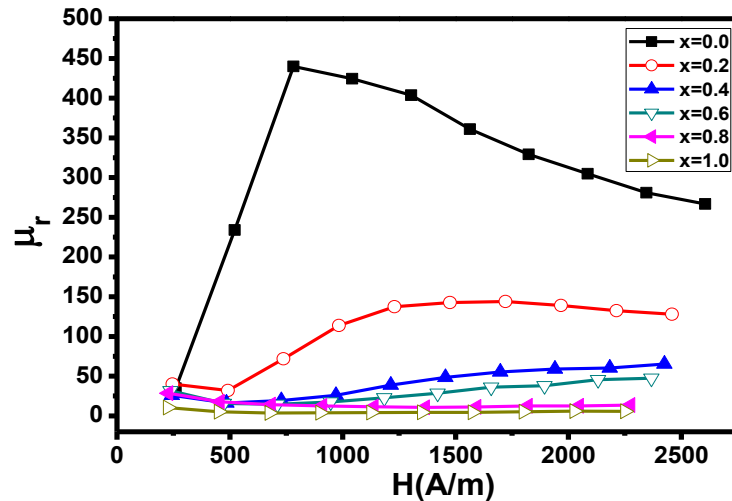


**Figure. (4.4):** Variation of  $\mu_r$  with  $H$  for the samples with  $x= 0.0, 0.2, 0.4, 0.6, 0.8$  and  $1.0$ .

## 4.2 Electric Properties

### Induction and Curie Temperature Point

The interested way to determine Curie temperature point ( $T_C$ ) of a ferrite is to measure the permeability ( $\mu$ ) of the ferrimagnetic materials which results from the domains walls motion and spin rotational (Shaah, 2012). It depends upon the magnetization, the ionic structure and the degree of domain walls continuity across the grain boundary layers (Dawoud and Shaah, 2006). It is found that  $\mu$  varies with different conditions such as the soaking time, the sintering temperature, the time of sintering, the porosity, the defects introduced and atmosphere of firing due to the sintering process (Shaah, 2012). The relation between the inductance ( $L$ ) of a closed packed coil (toroid) knitted around a substance and it's  $\mu$  is given by (Akhtar, Yahya and Hussain, 2009; Jebeli and Mohamed, 2013).

$$\mu = \frac{2\pi L}{N^2 l \ln\left(\frac{R_o}{R_i}\right)} \quad (4.6)$$

where  $N$  is the number of turns,  $R_i$  and  $R_o$  are inner and outer radii of toroid, respectively, and  $l$  is thickness of toroid. The permeability of the substance can, also, be expressed by:

$$\mu = \mu_o \mu_r \quad (4.7)$$

where  $\mu_r$  is the relative permeability. However,  $\mu_r$  at low excitation level and constitutes the most important means for the comparison of soft magnetic materials can be defined as the initial permeability ( $\mu_i$ ). Therefore, an expression for the initial permeability can be derived as follows

$$\mu_i = \frac{2\pi L}{\mu_o N^2 l \ln\left(\frac{R_o}{R_i}\right)} \quad (4.8)$$

The  $M$  of a specific core material located inside the coil has the following expression (Shaah, 2012; Nabiyouni, Fesharaki, Mozafari and Amighian, 2010).

$$M = \chi_m H = \frac{(\mu_i - 1)}{4\pi} H \quad (4.9)$$

where,  $\chi_m$  is the magnetic susceptibility,  $H$  is the magnetic field produced by the coil. By using equations (4.8) and (4.9), it can be found that

$$M = \left[ \frac{L}{2\mu_o N^2 l \ln\left(\frac{R_o}{R_i}\right)} - \frac{1}{4\pi} \right] H \quad (4.10)$$

It is clear from equation (4.10) that,  $M$  is proportional to  $L$ . This means that, if  $L$  changes with temperature,  $M$  also changes. Therefore, the transition or Curie temperature can be measured from the variation of  $L$  with temperature. The variation of  $L$  for the toroidal shape samples of mixed Li-Ni spinel ferrites have been investigated from room temperature to fit beyond the  $T_C$ . Figure (4.5a and 4.5b) gives a plot of  $L$  versus temperature, it can be seen that, the value of  $L$  increases with increasing of temperature up to a certain temperature  $T_C$ . At this point a sharp drop of  $L$  was occurred, proving that at this point the sample is changed from ferrimagnetic to paramagnetic. The  $T_C$  for the given spinel ferrite samples are depicted in figure (4.6). From this figure, it is noticed that  $T_C$  is decreased with increasing of  $x$  i.e. increasing of  $Ni^{2+}$  ions. The same behavior was also observed by other workers (Venkataraju, Sathishkumar and Sivakumar, 2010). This is attributed to the addition of the  $Ni^{2+}$  ions that replace the  $Fe^{3+}$  ions at the  $O_h$  sites, thus; the number of the  $Fe^{3+}$  ions decreasing at the  $O_h$  sites. This tends to decrease the strength of  $T_d$  and  $O_h$  exchange interactions of the type  $Fe_T^{3+} - O^{2-} - Fe_O^{3+}$ , apart from decreasing number of bonds or linkages between the magnetic ions [Gillfo, 1958].

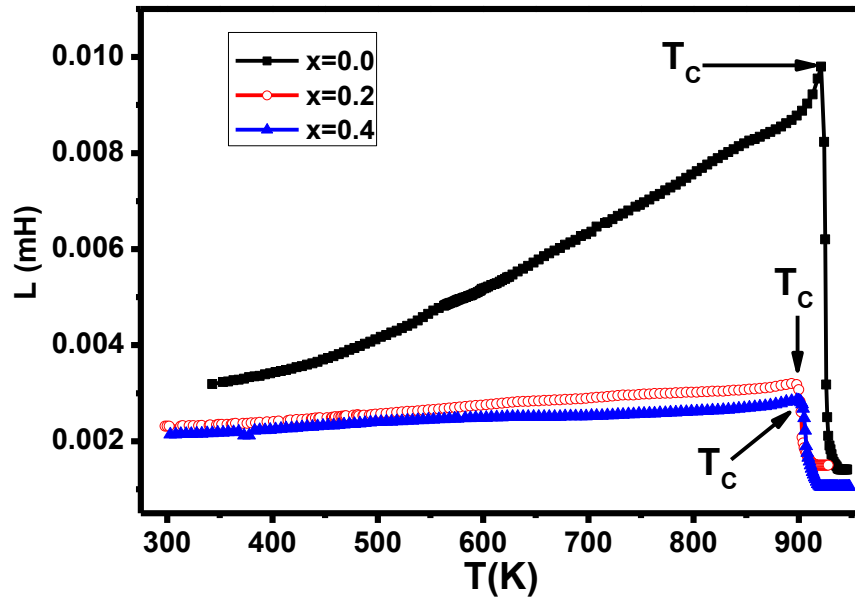


**Figure (4.5a):** Variation of induction  $L$  with temperature for samples of  $x = 0.0, 0.2$  and  $0.4$ .

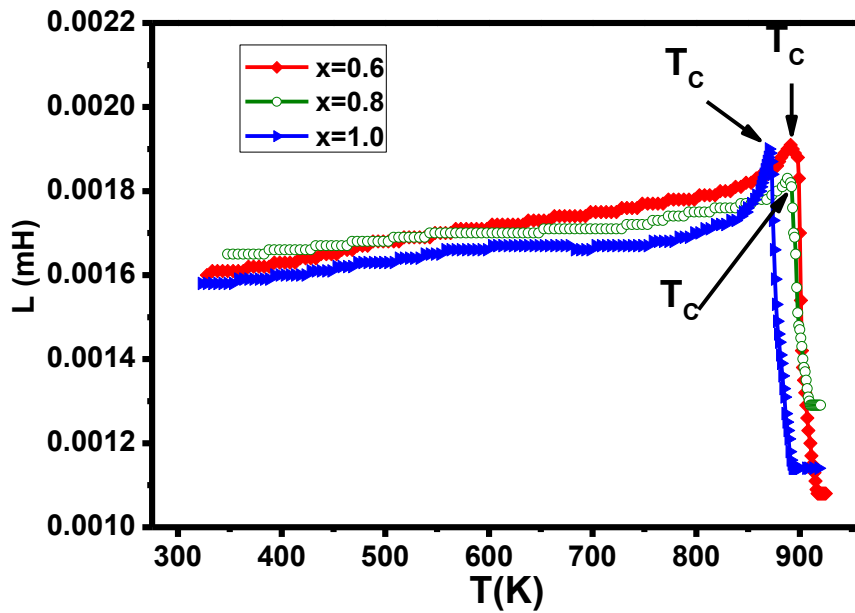
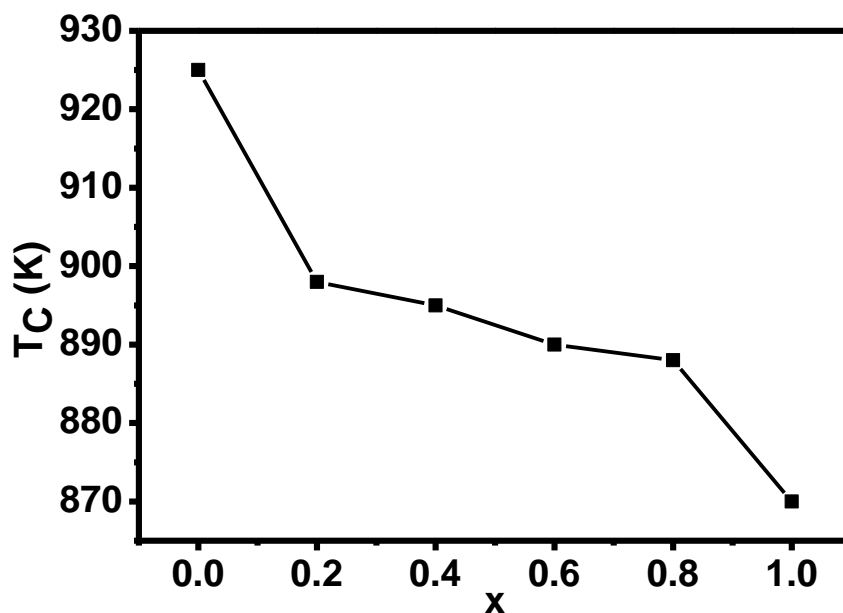


**Figure (4.5b):** Variation of induction  $L$  with temperature for samples of  $x = 0.6, 0.8$  and  $1.0$ .



**Figure(4.6):** Variation of  $T_C$  with  $Ni^{2+}$  ions concentrations (x).

### 4.3 Dielectric Properties

The frequency dependence of the complex dielectric constants ( $\epsilon^*$ ) for all prepared samples is shown in Figure (4.7). From this Figure, it can be seen that, the absolute value of  $\epsilon^*$  shows dispersion with increasing of the applied frequency which is a normal behavior for spinel ferrites that were studied by several investigators (Azadmanjiri , 2008; Ramesh, Craig, Dinesh,Rustum and Yadoji , 2003; Kumar, Kumar and Venudhar, 2012; Krishna et al, 2012; Chavan et al, 2013; Devmunde et al, 2016; Soibam, 2016). As indicated in the Figure (4.7) , the value of  $\epsilon^*$  is high at low frequencies but decreases rapidly with increasing of the applied frequency. The decrease in the  $\epsilon^*$  can be explained on the basis of space charge polarization and Koop's two layer model (Koops, 1951). According to this model, ferrite is assumed to be made up of well conducting grain separated by grain boundaries. The electrical conduction in ferrite is explained by Verwey mechanism in terms of the hopping of electrons between  $Fe^{2+}$  and  $Fe^{3+}$  ions at  $O_h$  sites (Verwey, Haayman and Romeijn ,1947). The electrons reach the grain boundary by hopping and pile up due to its higher resistivity. This produces the space charge polarization. In the present study, the substitution of  $Ni^{2+}$  ions



produce a change in the polarization so developed. There is a decrease in  $Fe^{3+}$  ions and increase in  $Ni^{2+}$  ions at the  $O_h$  site with increasing of Ni content. However, compared to  $Fe^{2+} \rightarrow Fe^{3+}$ , the exchange process of  $Ni^{2+} \rightarrow Ni^{3+}$  is weak. Hence, it is assumed to be the dominant mechanism (Smit and Wijn, 1959).

The decreasing in  $Fe^{3+}$  ions at the  $O_h$  site, therefore, decreases the hopping motion of electrons. This in turn decreases the piling up of electrons at the grain boundary, hence impeding the buildup of space charge polarization. Thus, the value of  $\epsilon^*$  decreases. At low frequency of applied field, the high resistivity grain boundary hinders the hopping motion of electrons creating space charge polarization, leading to a high dielectric constant. As the frequency of the applied field is increased, the electronic exchange is not able to follow the alternating field and the electrons reverse the direction of motion thus decreasing the probability of electrons reaching the grain boundary. This leads to a decrease in the value of  $\epsilon^*$ . At still higher frequency, the polarizability is very small and becomes independent of frequency. A similar behaviour was also observed at various ferrite systems (Sorokhaibam et al, 2015; Aravind et al, 2015).

Figure (4.8) shows the variation of dielectric loss tangent ( $\tan \delta$ ) with the same range of frequency. It can be seen that it has the same trend as  $\epsilon^*$ . It decreases with increase in frequency and becomes constant up to  $f=1000$  KHz due to decreased polarization at high AC fields.

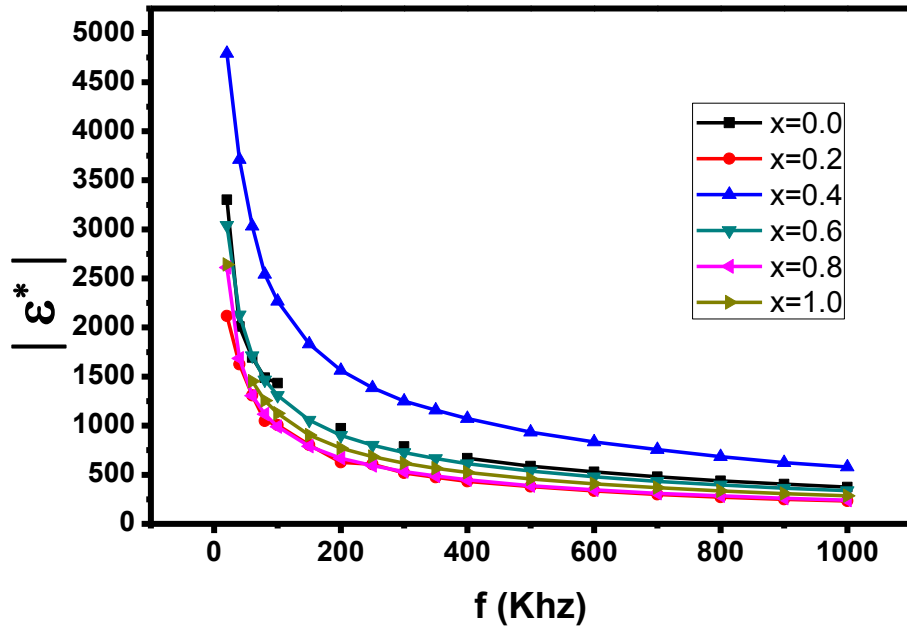


**Fig (4.7):** Variation of  $\epsilon^*$  against the applied frequency for the samples with  $x = 0.0$ , 0.2, 0.4, 0.6, 0.8 and 1.0 at room temperature.

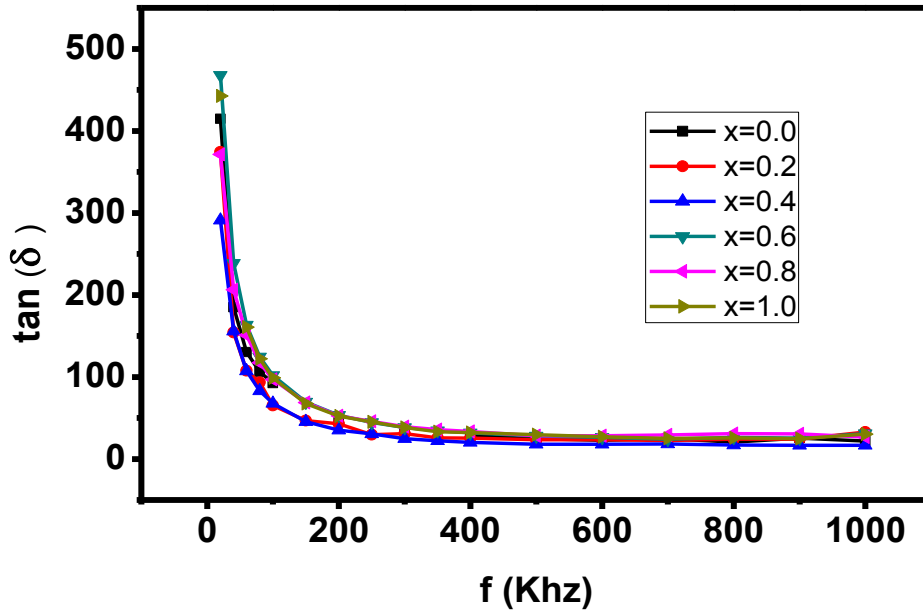


**Fig (4.8):** Variation of  $\tan \delta$  against the applied frequency for the samples with  $x = 0.0$ , 0.2, 0.4, 0.6, 0.8 and 1.0 at room temperature

#### 4.4 AC Conductivity:

The variation of the AC electrical conductivity ( $\sigma_{AC}$ ) with the applied frequency in the range of  $10^4 \text{ Hz}$  up to  $10^6 \text{ Hz}$  was studied at room temperature for the samples of  $Li_{.5-.5x}Ni_xFe_{2.5-.5x}O_4$  spinel ferrite. As shown in Figure (4.9),  $\sigma_{AC}$  for the introduced samples shows a continuous increasing with the increasing of the applied frequency. All samples exhibit normal behavior with the variation of the applied frequency. Due to the increasing in the applied frequency, the  $\sigma_{AC}$  of the investigated samples shows an increase because of the applied force driven by the frequency, which helps in transferring the charge carriers between the different conduction states. The behavior of the dispersion is associated with  $Ni$  content in the prepared samples and is found to decrease as increasing of  $Ni$  concentration. The same trend for spinel ferrites was confirmed from different workers (Shahjahan, Ahmed, Rahman, Islam and Khatun, 2014; Sekulic, Lazarevic, Sataric, Jovalekic and Omcevic, 2015; Dawoud, Shaat and Yassin, 2010).

It was found that,  $\sigma_{AC}$  for the  $Li-Ni$  spinel ferrite increase as the applied frequency increasing. This may be attributed to the electron hopping or the electron exchange, i.e.  $Fe^{3+} + e^- \Leftrightarrow Fe^{2+}$  or  $Ni^{2+} + h^+ \Leftrightarrow Ni^{3+}$  which occurs by the electron transform between the adjacent  $o_h$  sites in the spinel lattice (Shaat, 2012). However,  $\sigma_{AC}$  is increased is explained based on Verwey mechanism (Shaat, 2012). That is, the electron hopping may be occurred between the ions of the same element that present in more than one valence state and distributed randomly over crystallographically inequivalent lattice sites (Dawoud, A-Ouda and Shaat, 2016). Depending upon the sintering conditions, the number of such ions may be produced during the preparation of the ferrite samples. It is known that, partial reduction of the electron hopping,  $Fe^{3+} \Leftrightarrow Fe^{2+}$ , can take place at an elevated firing temperature (Shaat, 2012). Thus; the hopping of electron,  $Fe^{3+} \Leftrightarrow Fe^{2+}$ , occurs only by electron trans-form between the adjacent  $o_h$  sites in the spinel lattice at the highest frequency for all samples, it was found that, the sample with  $x = 0.4$  shows a rapidly increasing of  $\sigma_{AC}$ . This is because of the existence of a

maximum value of the divalent iron  $Fe^{2+}$  ions among all the mixed *Li-Ni* spinel ferrite, While for sample with  $x = 0.2$  the lowest value of  $\sigma_{AC}$  , This may be attributed to the lowest concentration of the  $Fe^{2+}$  ions among all the mixed *Li-Ni* spinel ferrite. A similar behavior was observed in various ferrite systems by several investigators (Dawoud et al, 2010; Alwash, Mohamad and Almaamori, 2016).

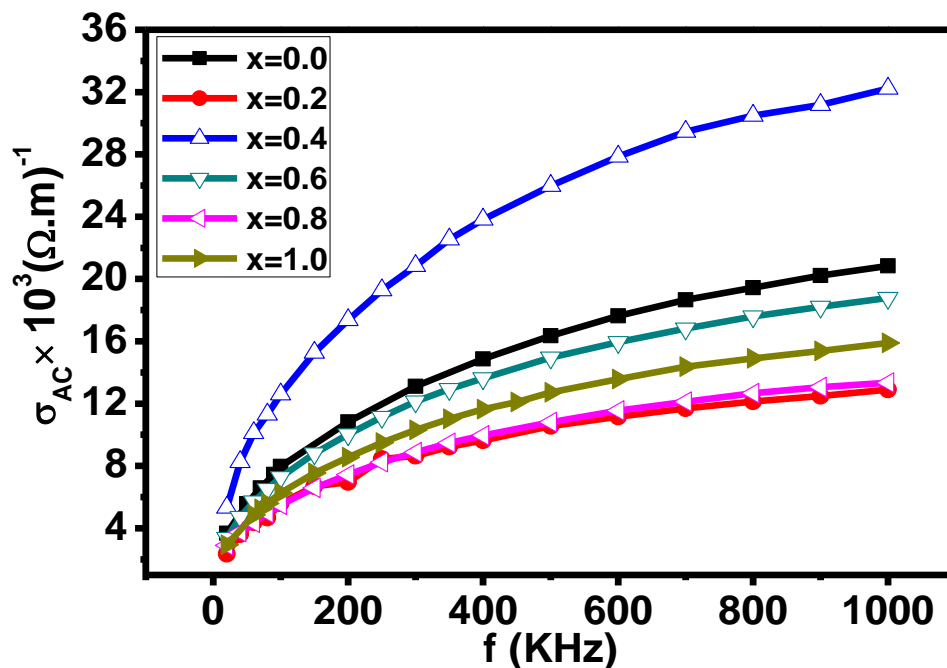


**Fig (4.9) :** Variation of  $\sigma_{AC}$  against the applied frequency for the samples with  $x = 0.0$ , 0.2, 0.4, 0.6, 0.8 and 1.0 at room temperature

# Conclusion

## Conclusion

Substitution of the  $Ni^{2+}$  ions in *Li* spinel ferrite has a tremendous influence such the magnetic, the electric and the dielectric properties. From this study, we concluded that:

- The net magnetic moment  $\mu_{net}$  and the magnetic moment of the octahedral site  $\mu_O$  of *Li-Ni* spinel ferrite were changed with increasing of the  $Ni^{2+}$  ions, while the magnetic moment of the tetrahedral site  $\mu_T$  remained constant .
- The ionic radius of the octahedral site  $R_O$  was changed linearly with increasing of the  $Ni^{2+}$  ions, while the ionic radius of the tetrahedral site  $R_T$  remained constant.
- The net magnetization was decreased with increasing of the  $Ni^{2+}$  ions for all the samples.
- The Curie temperature  $T_C$  was decreased with increasing of  $Ni^{2+}$  ions.
- The complex dielectric  $\epsilon^*$  was decreased with increasing of the applied frequency for all samples.
- The dielectric loss tangent  $\tan\delta$  was decreases with increasing of frequency and becomes constant up to  $f=1000$  kHz due to decrease polarization at high AC fields .
- The AC conductivity  $\sigma_{AC}$  was increased with increasing of the applied frequency.

Furthermore,  $Ni^{2+}$  content has significant influence on the electromagnetic properties, such as dielectric constant, dielectric loss tangent, electrical properties and magnetic properties for *Li* ferrites, so, the mixed *Li-Ni* spinel ferrite is considered a soft ferrite material, which is proved to be an interest material for technological and scientific applications.

# References

## References

- Albers, E. S. (1954). Ferrites for Microwave Circuits and Digital Computers. *J. Appl. Phys.*, 25, 152.
- Al-Shakarchi , E.K.(2015) Hydrothermal Method. *International Journal of Advanced Research in Physical Science (IJARPS)* ,2(9), 5-12.
- Alwash, N. H., Mohamad, H. K. and Almaamori, M. H. (2016). Effect of  $M^{2+}$  substitution on properties of the system  $Ni_xZn_{1-x-y}MyFe_2O_4$ . *International Letters of Chemistry, Physics and Astronomy*, 63, 42-48.
- A-Mosa ,Z.A.(2016). Improvement of electric and magnetic properties for Li spinel ferrite by divalent  $Zn^{2+}$  ions substitution. Faculty of Science the Islamic University–Gaza.
- Aravind, G., Raghasudha, M. & Ravinder, D. (2015). Electrical transport properties of nano crystalline Li–Ni ferrites. *J. of Materiomics*, 1, 348-356.
- Azadmanjiri,J. (2008). Structural and electromagnetic properties of Ni–Zn ferrites prepared by sol–gel combustion method, *Materials Chemistry and Physics*, 109, 109–112.
- Chavan, G. N., Belavi, P. B., Naik, L. R., Bammannavar, B. K., Ramesh, K. P. and Kumar, S. (2013). Electrical And Magnetic Properties Of Nickel Substituted Cadmium Ferrites. *International Journal of Scientific & Technology Research*, 82-89.
- Cheng, H., (1984). Modeling of electrical response for semiconducting ferrite. *J. Appl Phys.*, 56, 1831.
- Chikazumi, S. (1964). *Physics of Magnetism*. New York: John Wiley and Sons. Inc.
- Crangle, J. (1991). *Solid State Magnetism*. London: Edward Arnold.
- Dawoud, H., A-Ouda, L. and Shaat, S. K. K. (2016). Synthesize and Magnetic Properties of Ni Substituted Polycrystalline Zn-spinel Ferrites. *IJRASET*,4, 111-118.
- Dawoud, H. A., Shaat, S. K. K. and Yassin, S. S. (2010). AC Conductivity and Dielectric Properties of Cu–Zn ferrites. *Journal of Al Azhar University-Gaza (Natural Sciences)*,12, 65-74.
- Dawoud ,H., A-Ouda ,L. & Shaat, S. K. K. (2017). AC and Dielectric Properties of Polycrystalline Zn – Ni Spinel Ferrites Prepared by Double Sintering Technique.



*IUG Journal of Natural Studies Peer-reviewed Journal of Islamic University-Gaza*, 1-7.

- Dawoud, H. A. (1997). A study of Some Electric and Magnetic Properties of Li-Cu Spinel, Pd.D. Thesis, Faculty of Science Zagazig University, Egypt.
- Devmunde, B. H., Raut, A. V., Birajdar, S.D., Shukla, S. J., Shengule, D. R. and Jadhav, K.M. (2016). Structural, Electrical, Dielectric, and Magnetic Properties of Cd<sup>2+</sup> Substituted Nickel Ferrite Nanoparticles. *Journal of Nanoparticles*, 1- 8.
- Eatah, A., Ghani, A. A., & Faramawy, E. (1988). Effect of sintering temperature on the electrical conductivity and thermoelectric power of CuFe<sub>2</sub>O<sub>4</sub>. *Phys. Stat. Sol.*, 105, 231-233.
- Ferroxcube, (Jan. 2002). Soft Ferrite. Gorter, E. W. (1954). Saturation magnetization and crystal chemistry of ferrimagnetic oxides. *Philips Res. Rept*, 9, 295.
- Gillfo, M. A. (1958). Superexchange Interaction Energy for Fe<sup>3+</sup>-O<sup>2-</sup>-Fe<sup>3+</sup> Linkages. *APS Journals Archive*, 109, 777-781.
- Jadhav ,S.A. (2001). Magnetic Properties of Zn- substituted Li-Cu ferrites. *Journal of Magnetism and Magnetic Materials*, 224(2), 167-172.
- Khader A.S., Shariff S. M., Nayeem F., Basavaraja J., Madanakumara H. & Thyagaraj M. S. (2016). Structural and dielectric properties of Ni<sup>2+</sup> doped Chromium Ferrite by Solution Combustion method. *Journal of Chemical and Pharmaceutical Sciences*, 9(2), 993-997.
- Kittel, C. (1976). Introduction to Solid State Physics. (5<sup>th</sup> Edition). United States: John Wiley Sons.
- Klinger M. I. (1977). Electron conduction in magnetite and ferrites1. *J. phys. Stat. sol. B*, 79(1), 9-48.
- Klinger. M. I. (1975). Two-Phase Polaron Model of Conduction in Magnetite-Like Solids, *J. of Phys. C: Solid State Physics*, 8(21), 3595.
- Koop, G. G. (1951). On the Dispersion of Resistivity and Dielectric Constant of Some Semiconductors at Audio frequencies. *Phys. Rev.*, 83, 121.

- Krishna, K. R., Ravinder, D. K., Kumar, V., Joshi, U. S., Rana, V. A. and Lincon A. (2012). Dielectric Properties of Ni-Zn Ferrites Synthesized by Citrate Gel Method. *World Journal of Condensed Matter Physics*, 2, 57-60.
- Kulkarani, V. R., Todhar, M. M. & Vaingankar, A. S. (1986). Structural and Electrical Conductivity Studies in Nickel-Zinc Ferrite. *Ind. J. Pure Appl. Phys.*, 24, 294.
- Kumar, G. R., Kumar, K. V., Venudhar, Y. C. (2012). Electrical Conductivity and Dielectric Properties of Copper Doped Nickel Ferrites Prepared by Double Sintering Method. *IJMER*, 2(2), 177-185.
- Lafta, S.H., Al-Shakarchi, E.K., Musa, A.M., Farle, M. and Salikov, R. (2015). Effect of Molar Ratio on Structural Properties of Nanostructure Li-Ni Ferrites Prepared by Lax, B. & Button, K. J. (1962). *Microwave Ferrites and Ferrimagnetics*. New York: Mc. Grow-Hill.
- Lovell, M. C., Avery, A. J., Vernon, M. W. (1976). *Physical Properties of Materials*. New York: Van. Nostrand Reinhold Company.
- Mazen, S. A., Ghani, A. A. & Ashotr, A. H. (1985). Charge transport in Cu-Cd ferrosinels. *Phys. Stat. Sol.*, 88, 343–346.
- Moitgen, G., Angew, Z. (1952). *Phys. Rev.*, 4, 216.
- Morrish, A. H. (1965). *The Physical Principles of Magnetism*. United States: John Wiley and Sons. Inc.
- Neel, L. (1948). Propriétés magnétiques des ferrites. Ferrimagnétisme et antiferromagnétisme. *Ann. Phys.*, 3, 137-198.
- Nwanje, J. (1980). *J. Phys.* 3, 137-198.
- Nilima, N., Maisnam, M. & Phanjobam, S. (2015). Structural and Electrical Properties of Sol-gel Prepared Li-Ni-Co nanoferrites Sintered at Reduced Temperature. *International Journal of Engineering Innovation & Research*, 4(3), 415-418.
- Pathan, A.T. & Shaikh, A.M. (2012). Dielectric Properties of Co-Substituted Li-Ni-Zn Nanostructured Ferrites Prepared Through Chemical Route. *International Journal of Computer Applications (0975 – 8887)*, 45(21), 24-28.

- Patil, B. L., Sawant, S. R., Patil, S. A. & Patil, R. N. (1994). Electrical properties of  $\text{Si}^{4+}$  substituted copper ferrite. *J. Mat. Sci.*, 29, 175-178.
- Potakova, V. A., Zverv, N. D. & Romanov, V. P. (1972). On the cation distribution in  $\text{Ni}_{1-x-y}\text{FeZn}_y\text{FeO}_4$  spinel ferrites. *Phys. Stat. Sol. (A)*, 12(2), 623-627.
- Ramesh, P., Craig, G., Dinesh, A., Rustum, R. and Yadoji, P. (2003). Ultralow dielectric constant nickel–zinc ferrites using microwave sintering. *J. Mater. Res.*, 18(10), 2292-2295.
- Ravinder, D. & Latha, K. (1999). Dielectric behaviour of Mg-Zn ferrites at low frequencies. *Mat. Lett.*, 41, 247-253.
- Reddy, M. B. & Reddy, P. V. (1991). Low-frequency dielectric behaviour of mixed Li- Ti ferrites. *J. Phys. D: Appl. Phys.*, 24, 975-981.
- Rezlesus, N. & Rezlesus, E. (1974). Dielectric Properties of. Copper Containing Ferrites. *Phys. Stat. Sol.*, 23(2), 575-582.
- Rudden, M. N. & Wilson, J. (1984). Elements of Solid State Physics. United States: John Wiley and Sons.
- Sattar, A. A., El-Sayed, H. M. & Agami, W.R. (2007). Physical and Magnetic Properties of Calcium-Substituted Li-Zn Ferrite. *JMEPEG*, 16, 573–577.
- Say M. G. (1976). Alternating current machines (4<sup>th</sup>) Pitman Press.
- Sekulic, D. L., Lazarevic, Z. Z., Sataric, M. V., Jovalekic, C. D. and Omcevic, N. Z. (2015). Temperature-dependent complex impedance, electrical conductivity and dielectric studies of  $\text{MFe}_2\text{O}_4$  (M = Mn, Ni, Zn) ferrites prepared by sintering of mechanochemical synthesized nanopowders. *J Mater Sci: Mater Electron*, 26, 1291–1303.
- Serway, R. A. (1996). Physics for Scientists and Engineers with Modern Physics (6<sup>th</sup> ed.) Philadelphia: Saunders College Publishing.
- Shaat, S. K. K. (2012). *Advanced Ferrite Technology*. LAMBART.
- Shaat, S.K.K. (2004). Study of some electric and classic properties for Cu-Zn spinel ferrite Thesis, Faculty of Science the Islamic University–Gaza

- Shahjahan, M.D., Ahmed, N. A., Rahman, S. N., Islam, S. and Khatun, N. (2014). Structural and Electrical Characterization of Ni-Zn Ferrites. *IJETCAS.*, 13(104), 20-25.
- Smit, J. & Wijn, H. P. J. (1959). Ferrites, New York: John Wiley.
- Snelling, E. C. (1964). *Proc. Brit. Ceramic Soc. Z.*, 2, 151.
- Snelling, E. C. (1969). Soft Ferrites Properties and Applications, London: IIFFE.
- Snoek, J. L. (1947). New Developments in Ferromagnetic Materials. New York-Amsterdam: Elsevier Publishing Co., Inc.
- Soibam, I. (2016). A Study of Microwave Sintered Ni Substituted Lithium Zinc Ferrite Synthesized by Citrate Precursor Method. *International Journal of Materials Science and Engineering*, 4(1), 54-59.
- Sorokhaibam ,S., Soibam, I. & Phanjoubam, S. (2015) Dielectric Studies Of Li-Ni Ferrite Prepared By The Citrate Precursor Method. *International Journal of Materials Physics*, 6(1), 39-46.
- Standly, K. J. (1972). Oxide Magnetic Materials. United Kingdom: Clarendon Press.
- Tareev, B. (1975). Physics of Dielectric Materials. Moscow: C.M. Publishers.
- Tayal, D. C. (1998). Electricity and Magnetism. Himalaya Publishing House.
- Uitert, L. G. (1956). Dielectric Properties of and Conductivity in Ferrites. *J. of Chem. and Phys.*, 24,1294-1303.
- Venkataraju,C., Sathishkuma,G. & Sivakumar,K. (2010). Effect of nickel on the electrical properties of nanostructured Mn Zn ferrite.*Journal of Alloys and Compounds*,498(2), 203-206.
- Verwey, E. J. W. & Helimann, E. L. (1947). Physical Properties and Cation Arrangement of Oxides with Spinel Structures I. Cation Arrangement in Spinel. *J. Chem. Phys.*, 15, 174.
- Verwey, E. J. W., Deboer, F. & Vansanten, J. H. (1948). Cation Arrangement in Spinel. *J. Chem. Phys*, 16, 12.
- Verwey, E.J.W., Haayman, P.W. and Romeijn, F.C. (1947). Physical Properties and Cation Arrangement of Oxides with Spinel Structures II. Electronic Conductivity.*J. Chem. Phys.*, 15, 181-187.

Zaki H.M. (1992). A study of Electrical Properties of Li-Ge ferrite Spinel. Thesis submitted to the Faculty of Science Zagazig University, Egypt.